

The petrogenesis of Early Eocene non-adakitic volcanism in NE Turkey: Constraints on the geodynamic implications

Emre Aydinçakir *

Department of Geological Engineering, Gümüşhane University, TR-29000 Gümüşhane, Turkey



ARTICLE INFO

Article history:

Received 8 April 2014

Accepted 23 August 2014

Available online 7 September 2014

Keywords:

Non-adakitic volcanism

Slab break-off

 ^{40}Ar – ^{39}Ar geochronology

Artvin area

Eastern Pontides

NE Turkey

ABSTRACT

Whole-rock geochemistry, mineral chemistry, the ^{40}Ar – ^{39}Ar age, and Sr–Nd isotopic data are presented for the Early Eocene non-adakitic volcanic rocks on the eastern corner of the Eastern Pontides orogenic belt (NE Turkey). The tectonic setting of the Eastern Pontides during the Late Mesozoic to Early Cenozoic remains a topic of debate. Here, for the first time, we describe the Early Eocene non-adakitic volcanic rocks from the Eastern Pontides. These rocks contain plagioclase, hornblende phenocrysts, and magnetite/titanomagnetite and apatite microphenocrysts. Geochronology studies based on the ^{40}Ar – ^{39}Ar ratio of the amphibole separates reveal that the non-adakitic porphyritic volcanic rocks have a crystallization age of 50.04 ± 0.10 to 50.47 ± 0.22 Ma (Ypresian). The volcanic rocks show tholeiitic to calc-alkaline affinities and have low-to-medium K contents. They are also enriched in large-ion lithophile elements (LILE), light rare-earth elements (LREE), and depleted in high field strength elements (HFSE), with a no negative Eu anomaly ($\text{Eu}_n/\text{Eu}^* = 1.03$ –1.08) in mantle-normalized trace element spidergrams. The samples ($\text{La}_{\text{cn}}/\text{Lu}_{\text{cn}} = 2.60$ –4.28) show low-to-medium enrichment in LREEs relative to HREEs, in chondrite-normalized REE patterns indicating similar sources for the rock suite. These rocks display a range of I_{Sr} (50 Ma) values from 0.70451 to 0.70485, and $_{\text{Nd}}$ (50 Ma) 2.9 and 3.7. The main solidification processes involved in the evolution of these volcanics consist of fractional crystallization, with minor amounts of crustal contamination. All of our evidence supports the conclusion that the parental magma of the rocks probably derived from an enriched mantle, previously metasomatized by fluids derived from the subducted slab, in a post-collisional, geodynamic setting.

© 2014 Elsevier B.V. All rights reserved.

1. Introduction

The tectono-magmatic evolution of continent–continent collision systems consists of the generation of oceanic slab and its subduction, continent–continent collision, slab-break off, and delamination caused by crustal thickening. The chemical compositions of the melt in such a complex collision system are controlled by the unique phases of the system. Recent studies claim that Early Eocene magmatic activity in the Eastern Pontides exhibits adakitic character and is not widespread, although there is a large amount of Middle Eocene calc-alkaline magmatic activity in the region. In these studies, the Early Eocene magmatic activity has been assumed to be derived from the partial melting of lower crustal materials in response to a slab break-off process in the collision zone (Dokuz et al., 2013; Karsli et al., 2011; Topuz et al., 2005, 2011). In contrast, the Middle to Late Eocene magmatic activity is triggered by crustal thinning caused by continental extension (Arslan et al., 2013; Aslan et al., 2014; Aydinçakir and Şen, 2013; Temizel et al., 2012). However, Early Eocene non-adakitic volcanism

has not been reported in the region so far. By the term “non-adakitic” we refer to the andesitic porphyry rocks, which occurred at the same time interval with the adakitic rocks (57–50 Ma) but did not show much of the geochemical characteristics for those of the adakitic rocks of the region. Therefore, the petrogenetic and geodynamic processes of this magmatic activity are still being debated.

In this study, we present a dataset of whole-rock geochemical, mineral chemistry, Sr–Nd isotope data, and the ^{40}Ar – ^{39}Ar age of the Early Eocene non-adakitic volcanic rocks in the Artvin area to evaluate the tectono-magmatic and thermal history of the collision zone during the Early Cenozoic in the Eastern Pontides.

2. Geological setting

From Carboniferous to present, the Eastern Pontides orogenic belt is considered an example of well-preserved continental magmatic arcs. This tectonic unit comprises a mountain chain 200 km wide, extending along the southern Black Sea coast for 500 km. It occurs within the Alpine metallogenetic system. The Eastern Pontides is a subset of the Sakarya Zone, which is one of the major tectonic units of Turkey (Fig. 1a). The basement rocks of the Eastern Pontides are Carboniferous granitoids and Early Carboniferous metamorphic rocks (Delaloye et al.,

* Tel.: +90 4562337425; fax: +90 456 2337567.

E-mail address: emre@gumushane.edu.tr.

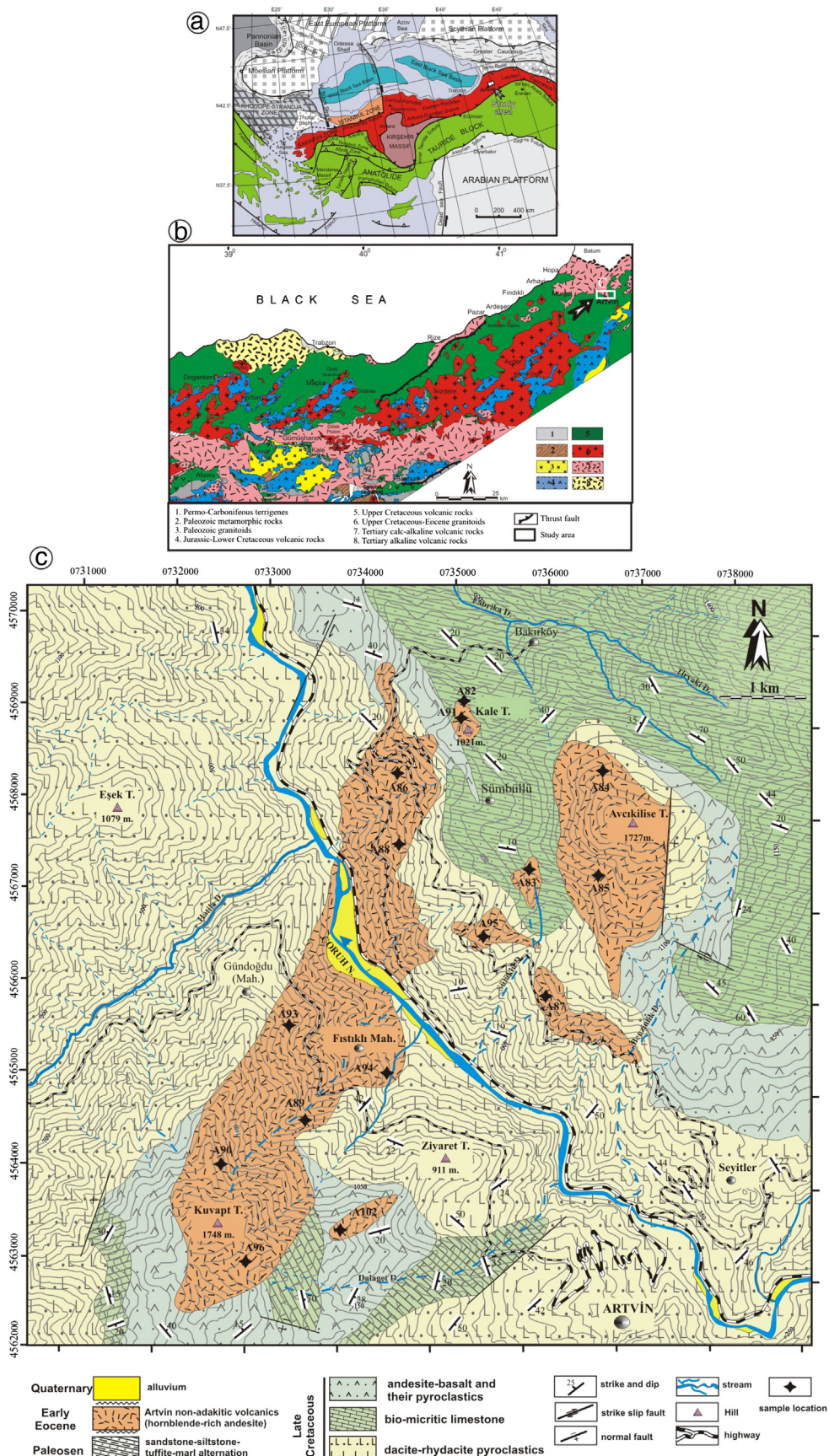


Fig. 1. (a) Regional tectonic setting of Turkey with main blocks in relations to the Afro-Arabian and Eurasian plates (modified from Okay and Tüysüz, 1999). (b) Simplified geological map of the Eastern Pontides (after the geological map with a scale 1:500,000; MTA, 2002). (c) Simplified geological map of the Artvin area showing the Early Eocene non-adakitic volcanic rocks with sample locations. Modified after Van (1990).

1972; Dokuz, 2011; Kaygusuz et al., 2012; Okay, 1996; Okay and Şahintürk, 1997; Topuz et al., 2007, 2010; Yilmaz, 1972; Yilmaz et al., 1997a, 1997b). Late Carboniferous to early Permian shallow marine to terrigenous sedimentary rocks accompany the granitoids (Çapkinoglu, 2003; Okay and Şahintürk, 1997). Late Triassic events are interpreted as associated with a subduction setting (Dokuz et al., 2010; Eyuboglu et al., 2011d; Karsli et al., 2014). The basement is overlain by early- and middle-Jurassic tuffs, pyroclastic and interbedded clastic and carbonate sedimentary rocks (Bektaş et al., 2001; Dokuz and Tanyolu, 2006; Kandemir, 2004; Kandemir and Yilmaz, 2009; Okay and Şahintürk, 1997; Şengör and Yilmaz, 1981; Yilmaz et al., 1997), and formations of basic volcanic rocks (Arslan et al., 1997; Genç and Tüysüz, 2010; Sen, 2007). Late Jurassic granitoids and their volcanic equivalents are emplaced into the volcano-sedimentary rocks of Şenköy Formation during middle-late Jurassic (Dokuz et al., 2010). The subduction polarity and geotectonic evolution of the Eastern Pontides are controversial at the Cretaceous. Some workers suggested that Eastern Pontides is a magmatic arc resulting in a northward subduction of the Neotethys along the southern border of the Sakarya Zone (Akin, 1979; Altherr et al., 2008; Karsli et al., 2010a; Okay and Şahintürk, 1997; Şengör et al., 2003; Ustaömer and Robertson, 2010). Conversely, Dewey et al. (1973), Bektaş et al. (1999) and Eyuboglu et al. (2011a,b) proposed a southward subduction continued uninterruptedly from Palaeozoic until the end of the Eocene. The magmatic arc is characterized by a more than 2-km thick volcano-sedimentary sequence with local intrusion of hornblende-biotite granitoids in the northern part of the Eastern Pontides (Boztuğ and Harlavan, 2008; Boztuğ et al., 2006; Kaygusuz and Aydinçakir, 2009, 2011; Okay and Şahintürk, 1997; Yilmaz and Boztuğ, 1996). The southern part introduces a fore-arc phase where flyschoid sedimentary rocks with limestone olistoliths were accumulated. The altitude of the Eastern Pontides (above sea level) during the Paleocene-Early Eocene era is attributed to the collision between the Pontides and the Tauride-Anatolide platform (Okay and Şahintürk, 1997; Şengör and Yilmaz, 1981). Post-Cretaceous magmatic rocks include Paleocene plagioclacites in the southern zone (Altherr et al., 2008). There are radiometric ages on this subduction which related high to ultrahigh potassic rocks from the western end of the Belt indicating the Late Cretaceous (Asan et al., 2014; Aydin, 2014; Eyüboğlu, 2010; Genc et al., 2014; Gülmез et al., 2014). Eocene volcanic and volcanoclastic rocks are intruded by calc-alkaline granitoids of a similar age (Arslan and Aslan, 2006; Eyuboglu et al., 2011a; Karsli et al., 2007, 2012). Early Eocene 'adakitic' granitoids (Eyuboglu et al., 2011b,c; Karsli et al., 2010a, 2011; Topuz et al., 2005, 2011), and Middle- to Late-Eocene calc-alkaline to tholeiitic, basaltic to andesitic volcanic rocks, as well as the cross-cutting granitoids were exposed throughout the Eastern Pontides (Arslan et al., 1997, 2013; Aslan, 2010; Aydinçakir and Sen, 2013; Kaygusuz et al., 2011; Temizel et al., 2012; Tokel, 1977). The Miocene and post-Miocene volcanic history of the Eastern Pontides is characterized by calc-alkaline to alkaline volcanism (Aydin et al., 2008; Dokuz et al., 2013; Eyuboglu et al., 2012; Sen et al., 1998; Yücel et al., 2014).

The Artvin area is located at the eastern-most Pontides in NE Turkey (Fig. 1a and b). The Late Cretaceous aged dacite, rhyodacite, and pyroclastics constitute the basement (Fig. 1c). It is conformably overlain by Late Cretaceous aged basalts and their pyroclastic equivalents intercalated with micritic limestone, sandstone, siltstone, and marl (Aydinçakir, 2012; Aydinçakir and Sen, 2013). This unit is conformably overlain by Paleocene aged sandstone, siltstone, marl and tuffite alternation. All of these units are cross-cut by the Early Eocene non-adakitic volcanic rocks (hornblende-rich andesite) (Fig. 1c). The coarse-grained hornblende-rich volcanic rocks are widely exposed as small, ellipsoidal bodies and/or dikes around Kale Tepe, Avcılık Tepe and Kuvapt Tepe located at the central part of the map area (Fig. 1c). All units are unconformably overlain by Quaternary alluvium (Fig. 1c).

3. Analytical techniques

3.1. Whole-rock major and trace element analyses

Based on the petrographical studies, 15 of the freshest and most representative rock samples from the volcanics were selected for major and trace element analyses. To prepare the rock powders, 0.5–1 kg of the fresh samples was crushed in a steel jaw crusher, and then the samples were ground in an agate mill to obtain grain sizes of <200 mesh. Major, trace, and REE elements were determined at the commercial ACME Analytical Laboratories Ltd, in Vancouver, Canada. The major and trace element compositions were measured by ICP-AES after 0.2 g samples of rock powder were fused with 1.5 g LiBO₂ and then dissolved via four acid digestion steps. The loss on ignition was determined by the weight difference after ignition at 1000 °C. The total iron concentration was expressed as Fe₂O₃. The detection limits are in the range of 0.001 to 0.1 wt.% for major element oxides, 0.1 to 10 ppm for trace elements, and 0.01 to 0.5 ppm for REE. Calibration and verification standards together with reagent blanks were added to the sample sequence. STD SO 18 was certified in-house against 38 certified reference material including CANMET SY-4 and USGS AGV-1, G-2, GSP-2 and W-2 as known external standards. The analytical accuracy is better than 4%.

3.2. Microchemical analyses

Electron microprobe analyses on polished thin sections were carried out at the New Mexico Institute of Mining and Technology, Socorro, NM, USA, using a Cameca SX-100 electron microprobe with three wavelength-dispersive spectrometers. Samples were examined using backscattered electron imagery, and selected minerals were quantitatively analyzed. Elements analyzed included F, Na, Mg, Al, Si, P, S, Cl, K, Ca, Ti, Cr, Mn, Fe, Sr, and Ba. An accelerating voltage of 15 kV and probe current of 20 nA were used, except for analyses using general glass labels (i.e., chlorite), which utilized a 10 nA probe current. Peak count numbers of 20 s were used for all elements, except for F (40 s; amphib/mica), F (60 s; glass), Cl (40 s), S (30 s), Sr (60 s), and Ba (60 s). Background count numbers were one-half the peak count times. A point beam of 1 μm was used to analyze amphibole, pyroxene, epidote, Fe-Ti oxide, and zircon. A slightly defocused (10 μm) beam was used to analyze feldspar, mica, and chlorite to avoid losses caused by sodium volatilization (Nielsen and Sigurdsson, 1981). Analytical results are presented in Supplementary Table 1.

3.3. Sr-Nd isotopic analyses

Isotopic analyses of Sr, Nd, and Pb were performed at the Department of Geological Sciences, New Mexico State University. All isotopic measurements were made by TIMS, on a VG Sector 30 mass spectrometer. All samples analyzed were loaded onto rhenium filaments on either Cathodian beads (single filament only) or on the side filament of a triple filament assembly. Reproducibility of the ⁸⁷Rb/⁸⁶Sr and ¹⁴⁷Sm/¹⁴⁴Nd ratios are within 0.3%, and the ⁸⁷Sr/⁸⁶Sr and ¹⁴³Nd/¹⁴⁴Nd ratios are within ± 0.000025 and ± 0.00003, respectively. An analysis of the NBS 987 standard yielded values of 0.710226 (11), 0.710213 (13), 0.710219 (10), and 0.710260 (11). Neodymium standards were unavailable and therefore not analyzed. Pb samples were analyzed using the middle filament position of a Cathodian bead assembly. Samples were loaded using 5% HNO₃ in a matrix of silica gel and phosphoric acid. Approximately 2 μL of silica gel was positioned on the filament and 1 μL of phosphoric acid was added. Standards were also loaded and analyzed using the same procedures. The mean of standard runs was ²⁰⁶Pb/²⁰⁴Pb = 16.844, ²⁰⁷Pb/²⁰⁴Pb = 15.379, and ²⁰⁸Pb/²⁰⁴Pb = 36.199. Deviations of the standards are within 0.2%. The detailed analytical procedures for Sr and Nd isotopic measurements are given in Ramos (1992).

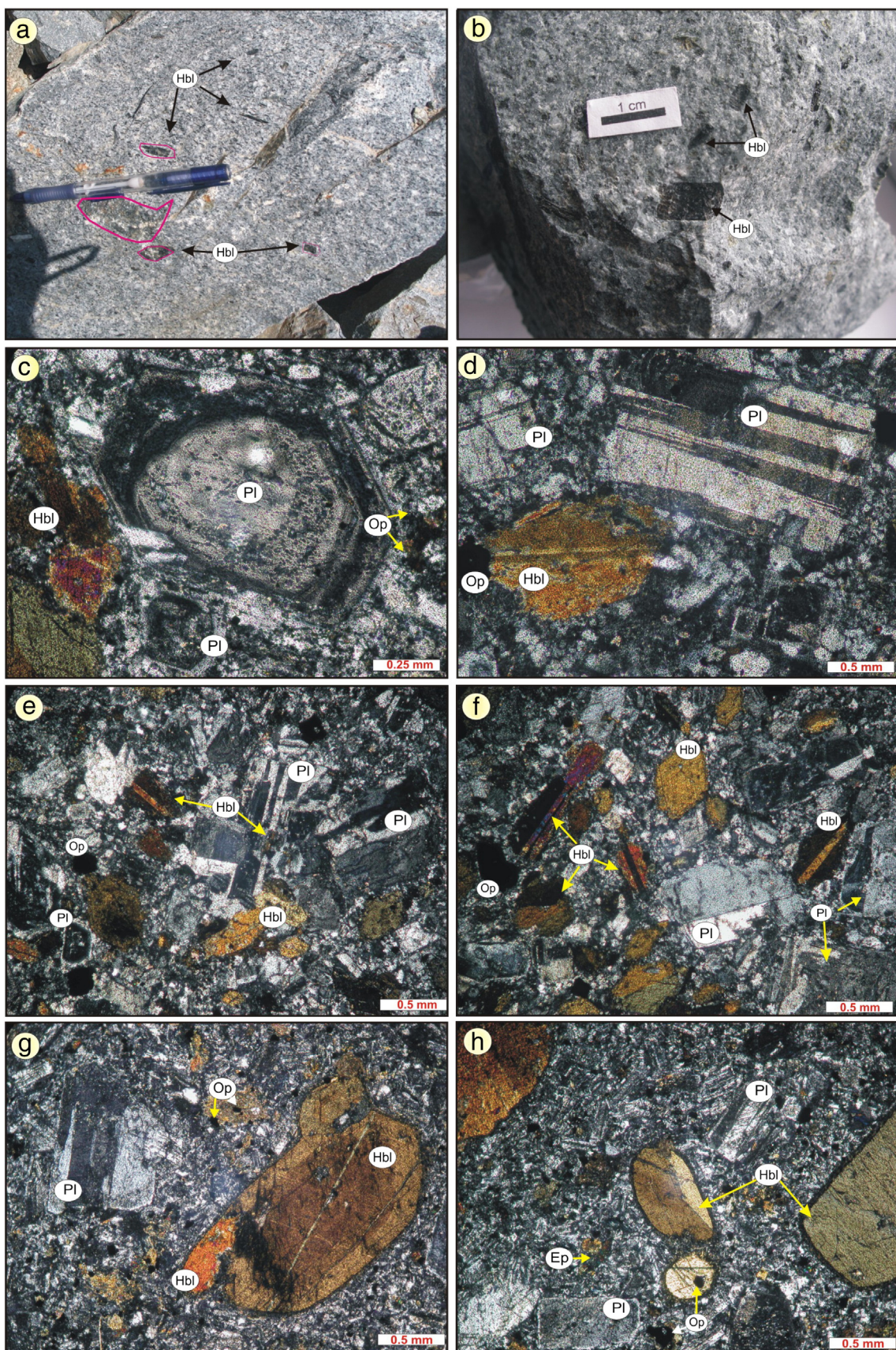


Fig. 2. Macrophotos of the (a–b) andesite. Microphotographs: (c) sieve texture and oscillatory zoned plagioclase phenocryst (Sample No: A-94, xpl), (d) albite twinned plagioclase and euhedral hornblende phenocryst (Sample No: A-94, xpl), (e) glomeroporphyric textures formed from plagioclase, hornblende and opaque minerals (Sample No: A-92, xpl), (f) euhedral hornblende phenocryst (Sample No: A-95, xpl), (g, f) zoned hornblende phenocrysts and rounded, embayed and opaque rims of the (Sample No: A-89, xpl). Symbols for minerals: Pl, plagioclase; Hbl, hornblend; Op, opaque; Ep, epidote, in the Early Eocene non-adakitic volcanic rocks.

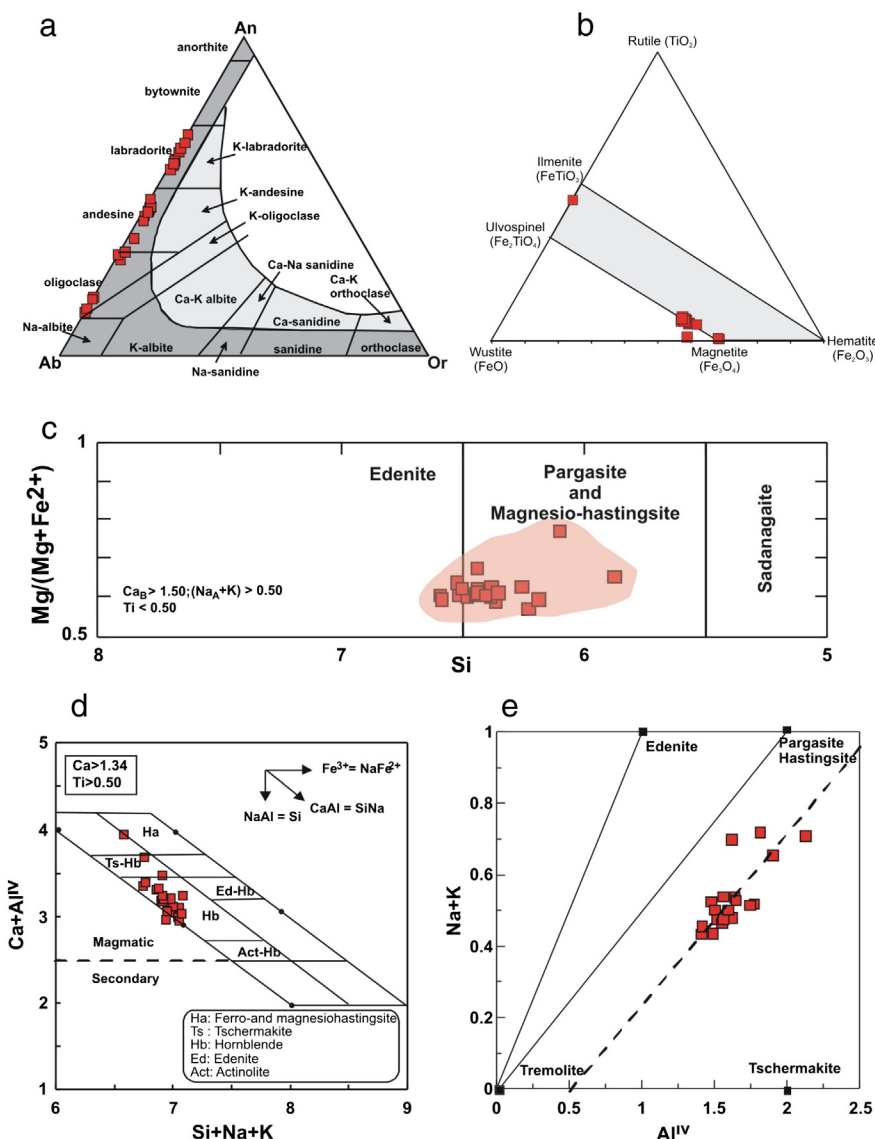


Fig. 3. (a) An-Ab-Or triangular plot showing the compositions of feldspars, (b) Fe-Ti oxide classification diagram (Bacon and Hirschmann, 1988), (c) classification of calcic amphiboles from the studied volcanics in the $Mg/(Mg + Fe^{2+})$ versus Si diagram (after Leake et al., 2004), (d) plot of amphibole composition in the $(Ca + Al^{IV})$ versus $(Si + Na + K)$ diagram (after Giret et al., 1980), (e) Substitution of amphiboles in the $(Na + K)^A$ versus Al^{IV} diagram (exchange vectors from Al'meev et al., 2002).

3.4. $^{40}\text{Ar}/^{39}\text{Ar}$ dating

$^{40}\text{Ar}/^{39}\text{Ar}$ incremental heating experiments were carried out in New Mexico Geochronology Research Laboratory at the New Mexico Tech University, USA. Whole rock reacted with dilute HCl followed by DI water rinse in an ultrasound. Fragments picked were free of phenocrysts. Hornblende separated by standard magmatic, heavy liquid and picking techniques. Samples were loaded into machined Al disk and irradiated for 8 h in the central thimble at the USGS reactor, Denver, CO. Neutron flux monitor Fish Canyon Tuff sanidin (FC-2). Assigned age = 28.201 Ma (Kuiper et al., 2008). ^{40}K decay constant $5.643 \times 10^{-10}/\text{a}$ (Min et al., 2000). Thermo-Fisher Scientific ARGUS VI mass spectrometer is in line with the automated all-metal extraction system. System = Obama Multi-collector configuration: 40Ar-H1, 39Ar-Ax, 38Ar-L1, 37Ar-L2, 36Ar-L3. Amplification: H1, L1, L2 1E12 ohm Faraday, AX 1E13 ohm Faraday, L3-CDD ion counter, deadtime 14 nS. Laser step-heating: samples step-heated with 75 W Photon-machines 810 nm diode laser. Reactive gases removed by 5 min reaction with 1 SAES GP-50 getters operated at 450 °C. Gas also exposed to cold finger operated at -140 °C and a W filament operated at ~2000 °C. Mass spectrometer

sensitivity = 1×10^{-16} mol/fA. Total system blank and background: $60 \pm 5\%$, $0.3 \pm 20\%$, $0.1 \pm 50\%$, $0.20 \pm 50\%$, $0.22 \pm 5\%$, $\times 10^{-17}$ moles for mass numbers 40, 39, 38, 37, and 36, respectively. J-factors determined to a precision of $\sim \pm 0.04\%$ by CO₂ laser-fusion of 6 single crystals from each of 6 radial positions around the irradiation tray. Correction factors for interfering nuclear reactions were determined using K-glass and CaF₂ and are as follows: $(^{40}\text{Ar}/^{39}\text{Ar})_{\text{K}} = 0.0072 \pm 0.00002$; $(^{36}\text{Ar}/^{37}\text{Ar})_{\text{Ca}} = 0.0002724 \pm 0.0000002$; and $(^{39}\text{Ar}/^{37}\text{Ar})_{\text{Ca}} = 0.00069 \pm 0.000002$.

4. Results

4.1. Petrography and mineral composition

These volcanic rocks are characterized, in hand specimens, by abundant euhedral to subhedral phenocrysts of plagioclase and amphibole, largely less than 1 cm in length, in whitish-gray and fine-grained groundmass observed (Fig. 2a and b). The samples were identified as a coarse-grained porphyritic hornblende andesite composition, petrographically. These volcanic rocks display porphyric, microlitic porphyric,

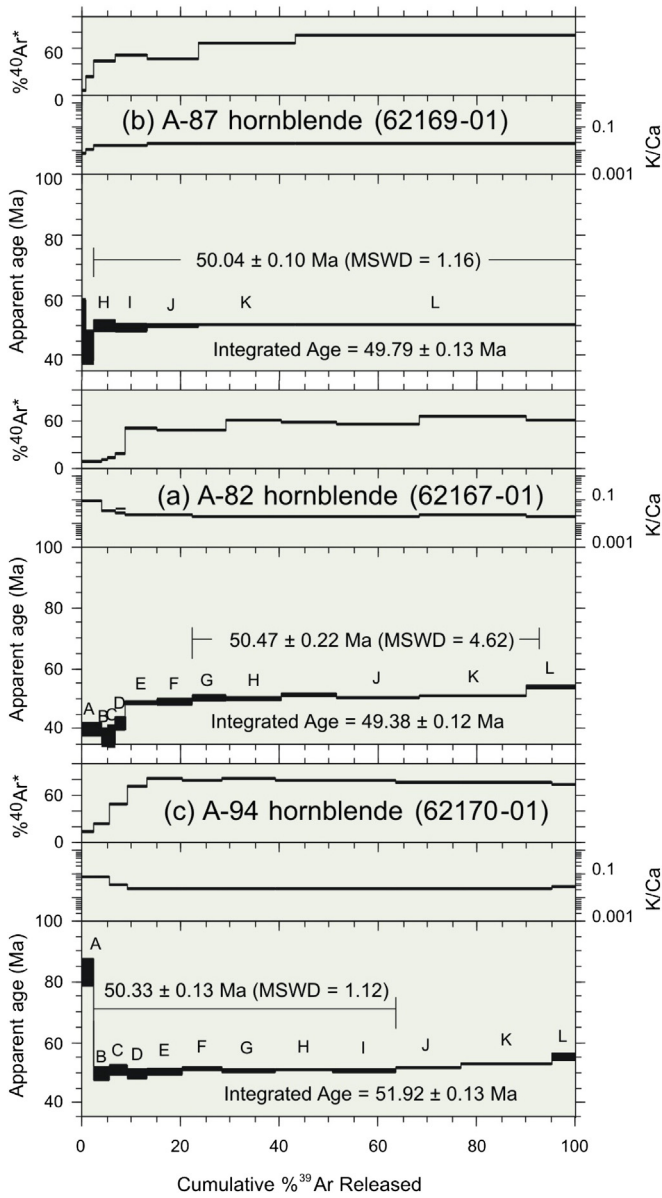


Fig. 4. Age, K/Ca and radiogenic yield diagrams of hornblende separates from the Early Eocene non-adakitic rocks. All errors quoted at 1 sigma.

glomeroporphyric and sieve textures (Fig. 2c–h) characterized by plagioclase and hornblende phenocrysts set in a groundmass of microlites of plagioclase, hornblende, Fe-Ti oxide and glass. All mineral compositional data are given in Supplementary Table 1 for Early Eocene non-adakitic volcanic rocks.

Plagioclases are present both as phenocrysts and microlites in the groundmass. They show a sieve texture, albite twinning, and oscillatory zoning, and occur as large euhedral to subhedral crystals. Some of the plagioclases contain hornblende and opaque minerals as inclusions and are altered into sericite. Plagioclase compositions range from An₁₄ to An₆₉ with oligoclase and labradorite (Fig. 3a and Supplementary Table 1).

Fe-Ti oxides are composed of ilmenite and titanomagnetite (Fig. 3b, Supplementary Table 1). Subhedral/anhedral Fe-Ti oxides are disseminated through the matrix. They also occur as inclusions in the hornblende and plagioclase phenocrysts (Fig. 2e and f).

Amphibole occurs as euhedral to subhedral phenocrysts and microlites in groundmasses. Phenocrysts (up to 2 mm) are common in

all rock types (Fig. 2g and h). In most instances, amphiboles are characterized by opaque rims and chloritization. Amphiboles have a $(\text{Ca} + \text{Na})^B$ content greater than 1.00, showing that they are calcic with a compositional variation in Si (5.87–6.59), Al (1.61–2.83), $(\text{Na} + \text{K})^A$ (0.43–0.72), and $\text{Al}^{VI} + \text{Fe}_{tot} + \text{Mg}$ (4.77–4.84). Following the nomenclature of Leake et al. (2004), hornblendes are classified as magnesio-hastingsite with $\text{Al}^{VI} < \text{Fe}^{3+}$ except for some hornblendes that are edenite (Fig. 3c). The Mg# of hornblendes vary from 0.57 to 0.77. Amphiboles are characteristically ferric with $\text{Fe}^{3+}\# = \text{Fe}^{3+} / (\text{Fe}^{3+} + \text{Fe}^{2+})$ ratios ranging between 0.51 and 0.85. All amphibole compositions with $(\text{Ca} + \text{Al}^{IV}) > 2.5$ plot in the field of magmatic amphiboles (Fig. 3d) proposed by Giret et al. (1980). The substitution mechanism (exchange vectors after Sakoma et al. (2000)) for the chemical composition of amphiboles is that of $\text{Ca} + \text{Al}^{VI} = \text{SiNa}$ (Fig. 3d). Amphiboles from volcanic rocks indicate a parallel trend for the pargasitic and hastingsitic substitution vectors in $(\text{Na} + \text{K})^A$ versus Al^{IV} plot (Fig. 3e).

4.2. ^{40}Ar - ^{39}Ar incremental heating dating

The results are given in Supplementary Table 2. Fig. 4 shows the results in the form of age spectra. The three hornblende separates yield ages of 50.04 ± 0.10 , 50.33 ± 0.13 , and 50.47 ± 0.22 Ma (Fig. 4), corresponding to the Early Eocene (Ypresian).

4.3. Whole-rock geochemistry

Geochemical data for the non-adakitic volcanic rocks are given in Table 1. The non-adakitic volcanic rocks are characterized by 55.34–63.52 wt.% SiO₂, 17.37–18.94 wt.% Al₂O₃, 4.21–6.75 wt.% Fe₂O₃_{tot}, 1.38–3.35 wt.% MgO, 304–546 ppm Sr, 12.5–16.2 ppm Y, 1.26–1.80 ppm Yb, and 3.7–15.1 ppm Rb (Table 1). Their Mg# numbers are between 39 and 51 (Table 1). In the total alkali-silica diagram (Fig. 5a), the rocks are classified as trachy-andesite, andesite, and dacite. This is further supported by the Zr/TiO₂ * 0.0001 versus Nb/Y diagram (Winchester and Floyd, 1977; Fig. 5b). In addition to this, due to mobility of Na₂O and K₂O, we classified the samples with the Co-Th diagram (Hastie et al., 2007). In this diagram, all the samples plot in calc-alkaline field (Fig. 5c).

This non-adakitic volcanic rocks fall into the normal arc andesite-dacite-rhyolite field with their relatively high Y (12.5–16.2 ppm) contents and low La/Yb (4–6) values on the Y versus Sr/Y and condrite-normalized Yb_n versus (La/Yb)_n diagrams (Fig. 6a and b).

The non-adakitic volcanic rocks display negative trends between SiO₂ and MgO, Fe₂O₃_{tot}, TiO₂ and Yb and relatively positive correlation with P₂O₅ and Al₂O₃. Although K₂O and Na₂O show scatter, they display an increasing trend with SiO₂ (Fig. 7). The variation observed above could reveal fractional crystallization processes. The increase in CaO and Al₂O₃ might suggest accumulation of feldspar and amphibole in the rocks. The scatter of K₂O and Na₂O for the samples could be related to alteration, but can also be related to the accumulation of plagioclase respectively in these rocks. Decreasing Fe₂O₃_{tot} and MgO with increasing SiO₂ are probably related to hornblende fractionation in the samples (Fig. 7). The volcanic rocks display variable enrichment in large ion lithophile elements (LILE), high field strength elements (HFSE), light rare earth elements (LREE), and heavy rare earth elements (HREE) with respect to primitive mantle and chondrite (Fig. 8a, b). The primitive mantle-normalized trace element distribution patterns of the rocks studied show enrichment in large ion lithophile elements (LILE; e.g., Rb, Th, K) relative to high field strength elements (HFSE) and also negative Nb, Ta, and Ti anomalies. Chondrite-normalized (Boynton, 1984) rare earth element patterns for the rocks studied show light rare earth element (LREE) enrichment with respect to heavy rare earth element (HREE) (La/Yb)_n ratios ranging from 2.61 to 5.51, with no significant Eu (mean Eu_n/Eu^{*} = 1.03–1.08) anomalies (Fig. 8c, d). These properties of rare earth elements of the rocks suggest that it is controlled by amphibole fractionation. The lack of any

Table 1

Whole-rock major and trace element compositions of Early Eocene non-adakitic samples from the Artvin area.

| Rock type | and | tr-and | tr-and | tr-and | tr-and |
|---|-------|-------|-------|-------|-------|-------|-------|-------|-------|-------|-------|--------|--------|--------|--------|
| Sample | A84 | A85 | A86 | A87 | A88 | A89 | A94 | A90 | A93 | A96 | A102 | A82 | A91 | A83 | A95 |
| SiO ₂ | 56.58 | 63.03 | 58.60 | 55.34 | 62.63 | 56.76 | 57.91 | 57.13 | 63.52 | 58.84 | 58.38 | 55.65 | 56.73 | 56.02 | 56.65 |
| TiO ₂ | 0.45 | 0.32 | 0.37 | 0.48 | 0.32 | 0.47 | 0.51 | 0.46 | 0.31 | 0.36 | 0.36 | 0.48 | 0.45 | 0.47 | 0.46 |
| Al ₂ O ₃ | 18.55 | 17.57 | 18.94 | 18.45 | 17.37 | 18.03 | 19.17 | 18.61 | 17.59 | 18.87 | 18.82 | 18.56 | 18.44 | 18.51 | 18.7 |
| Fe ₂ O ₃ ^{tot} | 6.34 | 4.26 | 5.48 | 6.75 | 4.23 | 6.22 | 6.65 | 6.35 | 4.11 | 5.28 | 5.42 | 6.66 | 6.25 | 6.44 | 6.32 |
| MnO | 0.16 | 0.17 | 0.18 | 0.16 | 0.17 | 0.14 | 0.16 | 0.16 | 0.17 | 0.18 | 0.18 | 0.15 | 0.17 | 0.15 | 0.17 |
| MgO | 2.99 | 1.38 | 2.14 | 3.35 | 1.42 | 3.21 | 3.20 | 2.97 | 1.45 | 2.13 | 2.20 | 3.32 | 2.91 | 3.31 | 3.09 |
| CaO | 5.88 | 5.23 | 7.17 | 8.25 | 5.23 | 8.18 | 8.71 | 5.81 | 4.75 | 7.13 | 7.07 | 5.45 | 5.08 | 5.38 | 5.27 |
| Na ₂ O | 5.09 | 4.53 | 3.81 | 2.96 | 4.46 | 2.93 | 3.17 | 5.16 | 4.48 | 3.75 | 3.75 | 5.76 | 6.15 | 5.83 | 5.86 |
| K ₂ O | 0.26 | 0.34 | 0.33 | 0.30 | 0.30 | 0.54 | 0.39 | 0.26 | 0.27 | 0.30 | 0.32 | 0.56 | 0.25 | 0.58 | 0.23 |
| P ₂ O ₅ | 0.12 | 0.19 | 0.14 | 0.11 | 0.19 | 0.14 | 0.12 | 0.12 | 0.18 | 0.13 | 0.14 | 0.12 | 0.12 | 0.11 | 0.12 |
| LOI | 3.4 | 2.9 | 2.7 | 3.6 | 3.5 | 3.2 | 1.3 | 2.8 | 3.0 | 2.9 | 3.2 | 3.1 | 3.3 | 3.1 | 3 |
| Sum | 99.80 | 99.89 | 99.88 | 99.81 | 99.85 | 99.83 | 99.82 | 99.83 | 99.87 | 99.87 | 99.85 | 99.81 | 99.81 | 99.86 | 99.84 |
| Mg# | 48 | 39 | 44 | 50 | 40 | 51 | 49 | 48 | 41 | 44 | 45 | 50 | 48 | 50 | 49 |
| Ni | 5.5 | 1.6 | 3.5 | 5.7 | 1.6 | 6.8 | 4.2 | 4.2 | 1.6 | 3 | 3.8 | 4 | 3.9 | 5.1 | 3.9 |
| Sc | 14 | 6 | 9 | 16 | 6 | 16 | 16 | 13 | 5 | 8 | 9 | 15 | 14 | 15 | 14 |
| Ba | 179 | 167 | 176 | 163 | 160 | 123 | 166 | 208 | 160 | 175 | 165 | 165 | 185 | 190 | 177 |
| Co | 13.2 | 4 | 7.4 | 14.8 | 4.6 | 13.5 | 14.7 | 13.7 | 4.8 | 8.9 | 9.2 | 14.3 | 12.6 | 15.2 | 13.9 |
| Cs | 1 | 0.5 | 0.3 | 0.6 | 0.4 | 0.3 | 0.4 | 1.2 | 0.5 | 0.3 | 0.2 | 0.6 | 1.1 | 0.8 | 1.1 |
| Ga | 17.7 | 14.3 | 15 | 16.3 | 15.1 | 17 | 17.9 | 17.2 | 16.3 | 16.3 | 16.4 | 16.5 | 17.4 | 17.5 | 16.7 |
| Hf | 1.7 | 2.2 | 2.3 | 1.6 | 2.3 | 1.6 | 2.1 | 1.6 | 2 | 1.9 | 2 | 1.8 | 1.5 | 1.8 | 2 |
| Nb | 1.9 | 3.5 | 2.4 | 2.4 | 2.7 | 2.6 | 2.1 | 2.6 | 2.8 | 2.6 | 2.3 | 2 | 2.1 | 2.3 | 2.2 |
| Rb | 3.7 | 9.8 | 6.1 | 6.2 | 9.9 | 15.1 | 10.3 | 4.7 | 9.9 | 6.7 | 6 | 12.6 | 3.9 | 14.1 | 4.6 |
| Sr | 486 | 428.7 | 395.2 | 337.5 | 407.7 | 313.7 | 304.3 | 522 | 442.2 | 409.8 | 391.9 | 311.5 | 526.8 | 333.5 | 545.5 |
| Ta | <0.1 | 0.2 | 0.1 | 0.1 | 0.1 | 0.1 | 0.1 | 0.1 | 0.2 | 0.1 | 0.1 | 0.1 | <0.1 | 0.1 | <0.1 |
| Th | 1.4 | 1.3 | 1.1 | 1.3 | 1.5 | 1 | 1 | 1.5 | 1.5 | 1.2 | 1.2 | 1.1 | 1 | 1.5 | 1.4 |
| U | 0.5 | 0.4 | 0.4 | 0.4 | 0.3 | 0.3 | 0.4 | 0.5 | 0.4 | 0.4 | 0.4 | 0.5 | 0.4 | 0.4 | 0.4 |
| V | 133 | 28 | 57 | 144 | 35 | 119 | 143 | 144 | 39 | 74 | 67 | 145 | 127 | 152 | 137 |
| Zr | 59.3 | 65.5 | 56.6 | 57.3 | 70.9 | 61.9 | 59.3 | 63.3 | 75.3 | 64.1 | 65.4 | 59.1 | 61.6 | 60.1 | 60.5 |
| Y | 13.4 | 12.5 | 13.3 | 14 | 12.7 | 14.4 | 16.2 | 13.4 | 13.2 | 13.6 | 14 | 13.4 | 13.6 | 13.7 | 13.8 |
| Cu | 27.2 | 2.5 | 8.4 | 23.2 | 1.6 | 18.9 | 28.9 | 32.4 | 1.1 | 8.4 | 7.9 | 25.3 | 26.5 | 33.2 | 30.7 |
| Pb | 3.1 | 1.8 | 2.1 | 2.2 | 1.6 | 1.6 | 1.1 | 2.7 | 1.2 | 1.7 | 1.9 | 4.6 | 3.2 | 2.7 | 3.2 |
| Zn | 44 | 76 | 41 | 44 | 53 | 26 | 24 | 48 | 58 | 35 | 34 | 47 | 37 | 53 | 43 |
| La | 7.7 | 10.3 | 8.2 | 7.8 | 9.4 | 7 | 7 | 8.7 | 10.7 | 8.5 | 7.4 | 7.5 | 8.1 | 8.6 | 8.9 |
| Ce | 15.2 | 21.5 | 17.1 | 15 | 20.4 | 15.5 | 14.9 | 17 | 21.6 | 17.4 | 17.2 | 15.1 | 16.3 | 16.7 | 17.2 |
| Pr | 1.98 | 2.61 | 2.16 | 1.96 | 2.66 | 1.97 | 1.99 | 2.07 | 2.75 | 2.3 | 2.18 | 1.89 | 2.05 | 2.01 | 2.11 |
| Nd | 7.7 | 10.9 | 8.5 | 7.4 | 10.2 | 8 | 8.5 | 9 | 11.8 | 9.7 | 9.2 | 7.3 | 7.7 | 8 | 8.9 |
| Sm | 1.84 | 2.34 | 2.24 | 1.85 | 2.27 | 1.98 | 2.07 | 1.89 | 2.33 | 2.14 | 2.12 | 1.73 | 1.8 | 1.85 | 1.88 |
| Eu | 0.65 | 0.78 | 0.77 | 0.67 | 0.75 | 0.7 | 0.75 | 0.67 | 0.8 | 0.79 | 0.76 | 0.64 | 0.64 | 0.65 | 0.67 |
| Gd | 1.84 | 2.1 | 2.07 | 1.99 | 2.14 | 2.05 | 2.33 | 2.07 | 2.23 | 2.29 | 2.14 | 1.91 | 1.97 | 2.12 | 2.05 |
| Tb | 0.34 | 0.34 | 0.35 | 0.36 | 0.34 | 0.36 | 0.4 | 0.33 | 0.32 | 0.35 | 0.37 | 0.34 | 0.34 | 0.33 | 0.33 |
| Dy | 2.12 | 2.02 | 2.53 | 2.28 | 1.97 | 2.45 | 2.43 | 2.31 | 2.1 | 2.32 | 2.11 | 2.21 | 2.17 | 2.23 | 2.27 |
| Ho | 0.42 | 0.38 | 0.46 | 0.46 | 0.39 | 0.48 | 0.53 | 0.45 | 0.45 | 0.45 | 0.42 | 0.45 | 0.43 | 0.42 | 0.48 |
| Er | 1.43 | 1.22 | 1.29 | 1.43 | 1.31 | 1.47 | 1.68 | 1.36 | 1.17 | 1.35 | 1.34 | 1.44 | 1.37 | 1.32 | 1.33 |
| Tm | 0.24 | 0.23 | 0.22 | 0.24 | 0.22 | 0.26 | 0.29 | 0.22 | 0.2 | 0.23 | 0.24 | 0.24 | 0.25 | 0.23 | 0.23 |
| Yb | 1.45 | 1.26 | 1.71 | 1.55 | 1.49 | 1.66 | 1.8 | 1.52 | 1.4 | 1.65 | 1.6 | 1.47 | 1.55 | 1.45 | 1.56 |
| Lu | 0.25 | 0.25 | 0.27 | 0.26 | 0.25 | 0.26 | 0.28 | 0.26 | 0.26 | 0.27 | 0.27 | 0.25 | 0.25 | 0.25 | 0.25 |
| Sr/Y | 36.3 | 34.3 | 29.7 | 24.1 | 32.1 | 21.8 | 18.8 | 39.0 | 33.5 | 30.1 | 28.0 | 23.2 | 38.7 | 24.34 | 39.53 |
| (La/Yb)n | 3.58 | 5.51 | 3.23 | 3.39 | 4.25 | 2.84 | 2.62 | 3.86 | 5.15 | 3.47 | 3.12 | 3.44 | 3.52 | 4.00 | 3.85 |
| (Yb)n | 6.94 | 6.03 | 8.18 | 7.42 | 7.13 | 7.94 | 8.61 | 7.27 | 6.70 | 7.89 | 7.66 | 7.03 | 7.42 | 6.94 | 7.46 |
| Eu/Eu* | 1.07 | 1.06 | 1.08 | 1.06 | 1.03 | 1.05 | 1.04 | 1.03 | 1.06 | 1.08 | 1.07 | 1.03 | 1.00 | 1.00 | 1.04 |

Rock types: and, andesite; tr-and, trachy-andesite; Mg# is $100 \times \text{MgO} / (\text{MgO} + 0.9\text{FeO}_{\text{tot}})$ in molar proportions. Oxides are given in wt.%, trace elements in ppm.

conspicuous positive or negative Eu anomaly indicates that neither plagioclase fractionation nor melting that left behind plagioclase-bearing residues was important in the generation of magmas for the Artvin area.

4.4. Whole-rock Sr–Nd isotope composition

The Sr and Nd isotopic compositions of four samples are listed in Table 2 and plotted in Fig. 9 together with the mantle array and the fields for MORB and adakites (Castillo, 2012), Early Eocene adakitic rocks from the Eastern Pontides, Turkey (Eyuboglu et al., 2011a,c; Karsli et al., 2010b, 2011; Topuz et al., 2005, 2011), and Eastern Pontides calc-alkaline volcanics (Arslan et al., 2013; Aydinçakir and Şen, 2013; Kaygusuz et al., 2011; Temizel et al., 2012). All of the samples show a small range of Sr–Nd isotope ratios with I_{Sr} (50 Ma) ranging from 0.70451 to 0.70485 and $^{143}\text{Nd}/^{144}\text{Nd}$ (50 Ma) ratios (0.51272–0.51276) corresponding to $\varepsilon_{\text{Nd}}(50 \text{ Ma})$ values from 2.9 to 3.7 (Fig. 9). The Nd

model ages (T_{DM}) of the samples are young and relative to the depleted mantle range from 0.69 to 0.84 Ga (Table 2). As illustrated in Fig. 9, the volcanic rocks are placed on the mantle array in the depleted quadrants of a conventional Sr–Nd isotope diagram. These values nearly correspond to those estimated for bulk earth, so they are similar to those of other volcanics of the Early Eocene adakitic rocks and the Middle Eocene calc-alkaline volcanics from Turkey.

5. Discussion

5.1. Petrogenesis of the non-adakitic volcanic rocks

The volcanic rocks present geochemical fingerprints typical for those of the subduction zone volcanic rocks, such as enrichment in LILE and LREE and negative Nb, Ta anomalies (Baier et al., 2008; Elburg et al., 2002; Pearce, 1983; Thompson et al., 1984). The most basic samples of

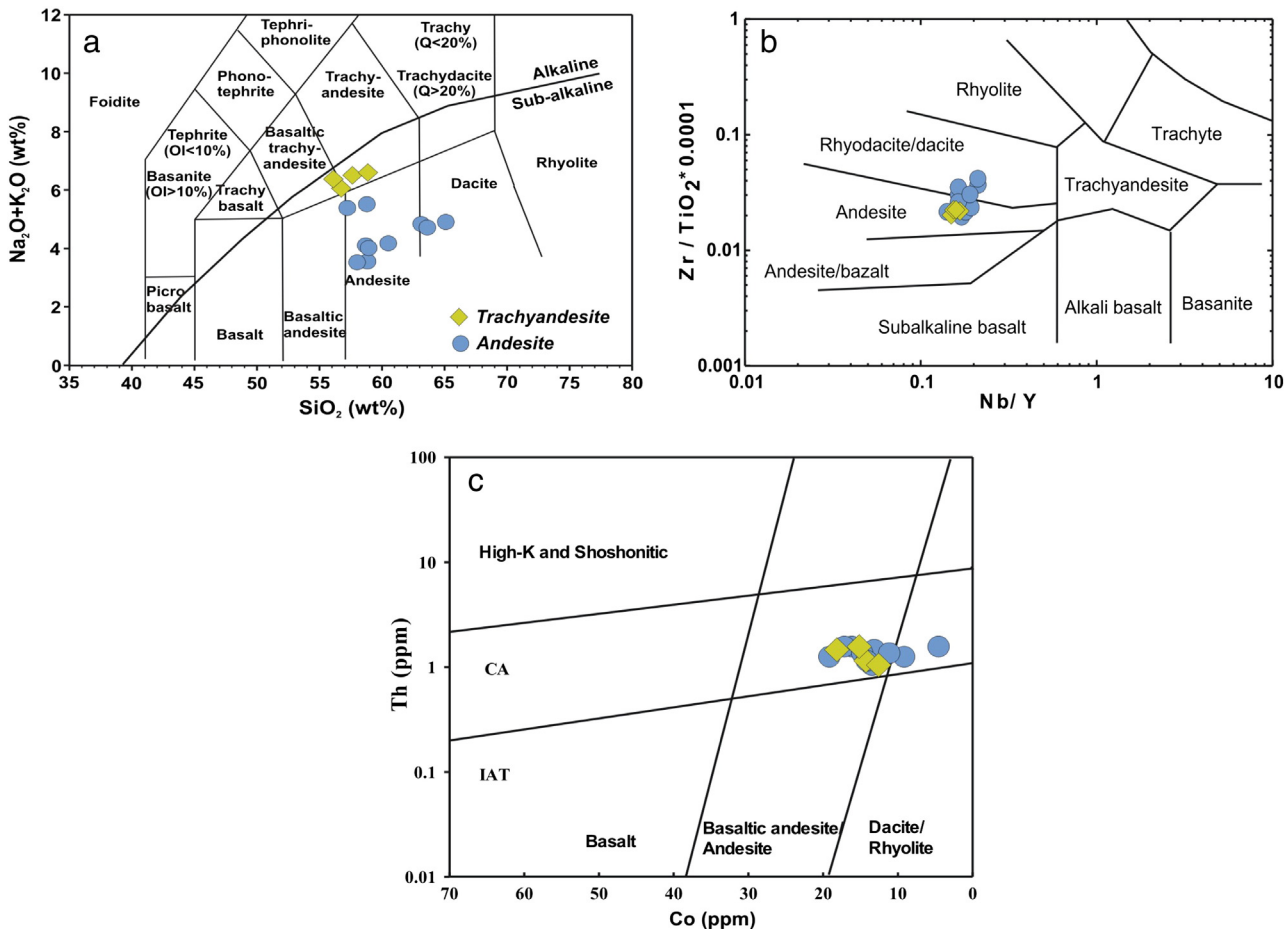


Fig. 5. Volcanic rocks on various geochemical classification diagrams. (a) $\text{Na}_2\text{O} + \text{K}_2\text{O}$ wt.% versus SiO_2 wt.% diagram (Le Bas et al., 1986), (b) $\text{Zr}/\text{TiO}_2 * 0.0001$ versus Nb/Y diagram (Winchester and Floyd, 1977), (c) Th (ppm) versus Co (ppm) (Hastie et al., 2007).

the rocks lack primitive rocks with $\text{Mg}\# > 70$ or high compatible element abundances—for example, $\text{Ni} > 200$ ppm, $\text{Cr} > 400$ ppm—that are considered to represent magmas derived directly from the peridotitic mantle (Tatsumi and Eggins, 1995). The geochemical Sr and Nd isotopic compositions of the volcanic rocks in the Eastern Pontides, provide constraints on the nature of the mantle source, the evolutionary processes of the parental magma, and the geodynamic setting. The principal evidence for such a generation is clearly illustrated below.

5.2. Magma evolution: fractional crystallization versus assimilation processes

The non-adakitic volcanic rocks have low Ni (1.6–6.8), Co (4–15.2), and $\text{Mg}\#$ (39–51) contents, suggesting that the most mafic samples of the volcanic rocks are not a product of primary magma. The Harker variation diagrams show that chemical trends may be consistent with fractional crystallization with minor contamination (Fig. 7). The lack of negative Eu anomalies in the most primitive samples (Fig. 8) indicates that plagioclase was not a major fractionating mineral phase.

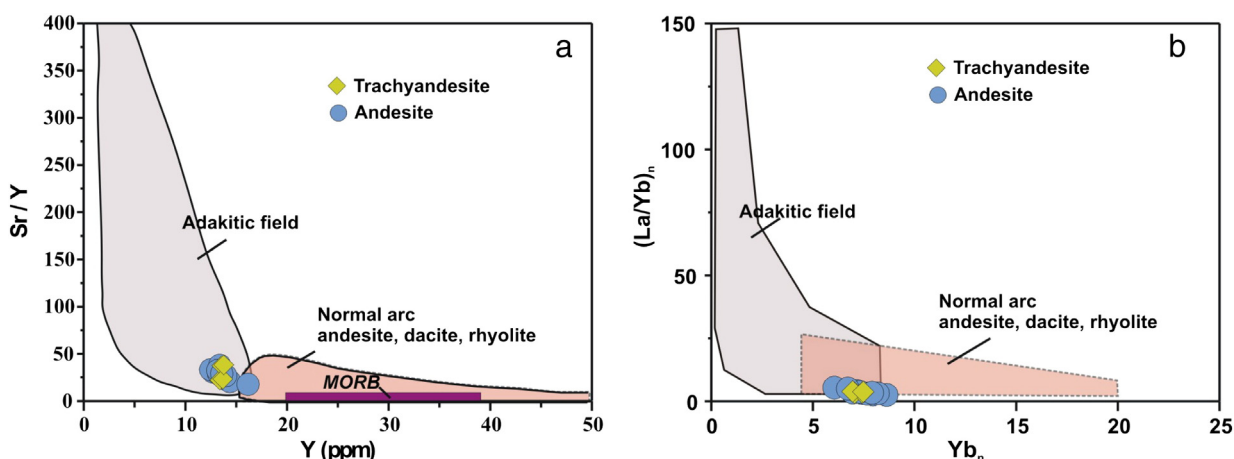


Fig. 6. Adakite discrimination diagrams (a) Y versus Sr/Y , and (b) Yb_n versus $(\text{La}/\text{Yb})_n$ (Defant and Drummond, 1990; symbols are as in Fig. 5a).

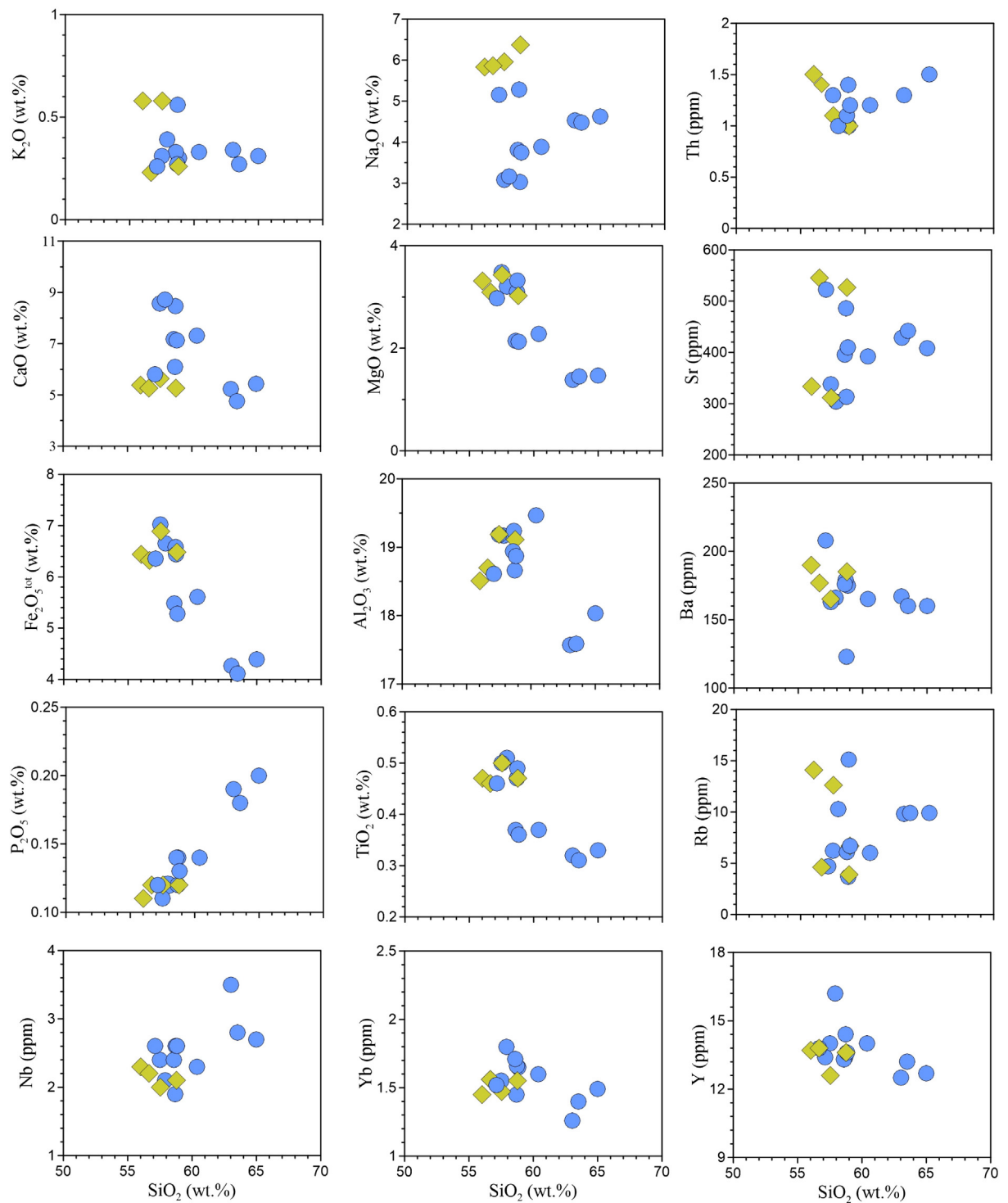


Fig. 7. Harker variation diagrams for the studied volcanic rocks (symbols are as in Fig. 5a).

Major and trace element compositions of the volcanic rocks indicate that hornblende \pm plagioclase \pm magnetite \pm apatite were important fractionating mineral phases in the petrogenesis of the rocks.

In calc-alkaline suites, Lambert and Holland (1974) used a CaO versus Y diagram to define J- and L-type trends, which lead to depletion and enrichment in Y relative to the calc-alkaline series standard, respectively. In the Y versus CaO diagram (Fig. 10), nearly all of the rocks plot on the Y-depleted side of the standard calc-alkaline trend, defined as a J-type trend. This trend implies that hornblende played an important

role in the evolution of the volcanic rocks. In the Sr and Nd isotopic diagram, the volcanic rocks plot between MORB and bulk silicate Earth (Fig. 9) isotopic ratios. This is not consistent with extensive crustal contamination.

The variation in Ti, Zr, Y, and V within the suite of arc rocks is clearly related to the nature and proportion of crystallizing phases (Pearce and Norry, 1979). The SiO₂ versus Sr/Y diagram appears generally to be a result of plagioclase fractionation (Fig. 11a). The crystallization of V and Fe-Ti oxides within volcanic rocks is reflected by a trend of decreasing

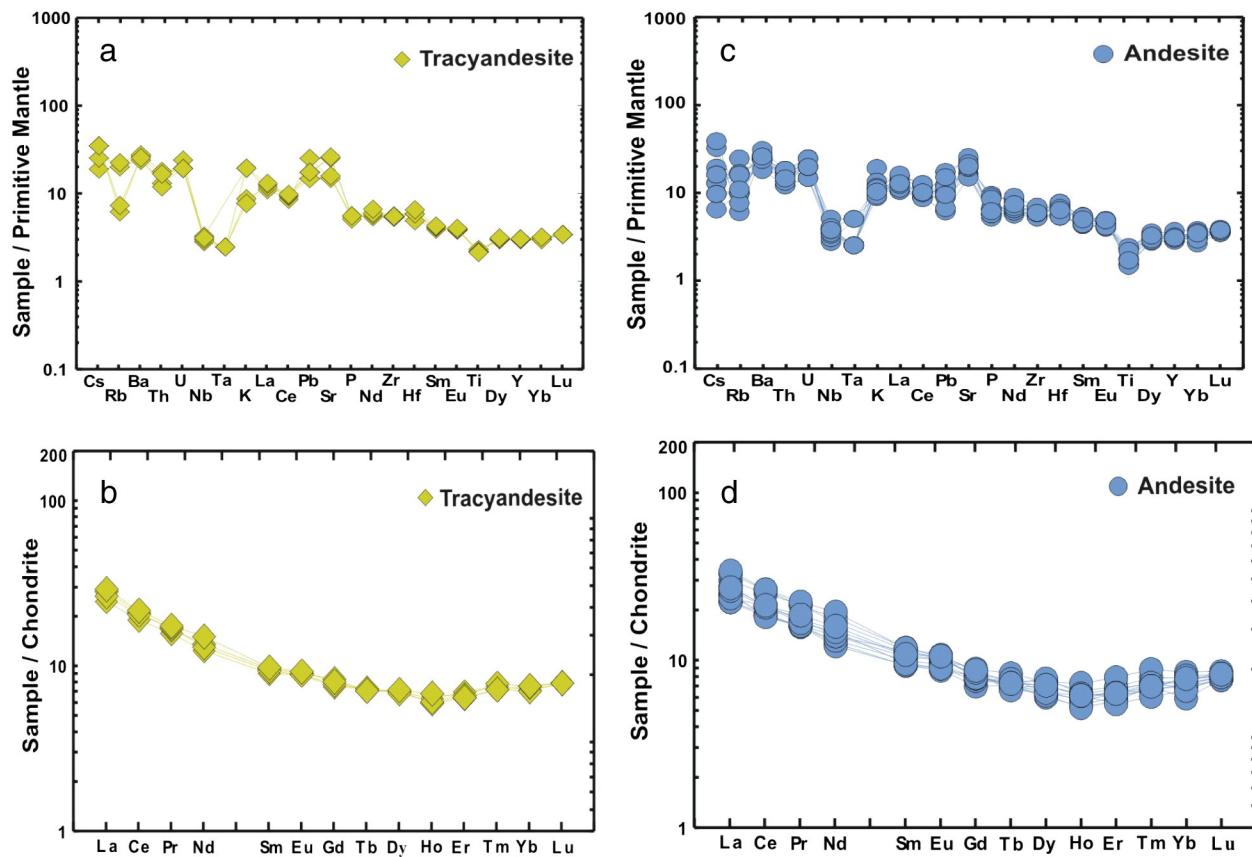


Fig. 8. Primitive mantle-normalized multi-element abundances (a, b) and chondrite-normalized REE patterns (c, d). The PM values are from Sun and McDonough (1989) and chondrite values are from Boynton (1984), (symbols are as in Fig. 5a).

Ti/Zr and V/Ti for residual melts (e.g., Nielsen et al., 1994; Pearce and Norry, 1979). The Zr concentrations appear to be controlled almost exclusively by fractionation. Zirconium enrichment relative to Sm is often attributed to amphibole fractionation (Thirlwall et al., 1994). Moreover, magnetite fractionation (Tribuzio et al., 1999) may also exert an influence on the Zr/Sm ratio.

Many studies on arc magmatism confirm the importance of crustal assimilation, which leads to changes in the trace elements present and the isotopic composition of mantle-derived arc magmas (Thirlwall et al., 1996). Arslan et al. (2013) and Aydinçakir and Şen (2013) argued for the contamination of the primary melt by mature and thickened arc crusts as an important feature of post-collisional Tertiary magmatism in the Eastern Pontide belt. The composition of these rocks was mainly modified by fractional crystallization rather than by AFC. In Fig. 12, the $I_{\text{Sr}}(50 \text{ Ma})$, and $\varepsilon_{\text{Nd}}(50 \text{ Ma})$ ratios are plotted against SiO_2 , MgO , Th ,

and $1/\text{Sr}$ to evaluate the role of fractional crystallization (FC) or the AFC processes. The plot of La/Yb ratios versus La contents may be consistent with the suggestion that the partial melting process was controlled the compositional variation. Positive or negative trends attest to the fact that the magmas were affected by AFC processes, whereas nearly constant trends indicate significant crystallization.

5.3. Source characteristics

The non-adakitic volcanic rocks are characterized by enrichments in LILE and LREE. Negative Nb, Ta, and Ti anomalies are features of subduction-related magmas and are commonly attributed to a mantle wedge source that was modified by metasomatic fluids derived from subducted slab or sediments (Cameron et al., 2003; Hawkesworth et al., 1991; Münker et al., 2004; Ringwood, 1990).

Table 2

Sr and Nd isotope data for the Early Eocene non-adakitic volcanic rocks from the Eastern Pontides.

| Sample | Rb (ppm) | Sr (ppm) | $^{87}\text{Rb}/^{86}\text{Sr}$ | $^{87}\text{Sr}/^{86}\text{Sr}$ | 20m | I_{Sr} (50 Ma) | Sm (ppm) | Nd (ppm) | $^{147}\text{Sm}/^{144}\text{Nd}$ | $^{143}\text{Nd}/^{144}\text{Nd}$ | $(^{143}\text{Nd}/^{144}\text{Nd})_i$ (50 Ma) | 20m | $\varepsilon_{\text{Nd}}(0)$ | ε_{Nd} (50 Ma) | T_{DM}^* (Ga) |
|-----------------------|-------------|-------------|---------------------------------|---------------------------------|-----|----------------------------|-------------|-------------|-----------------------------------|-----------------------------------|--|-----|------------------------------|--------------------------------------|---------------------------|
| <i>Trachyandesite</i> | | | | | | | | | | | | | | | |
| A82 | 12.6 | 312 | 0.0404 | 0.704938 | 11 | 0.70485 | 1.73 | 7.30 | 0.1439 | 0.512812 | 0.512764 | 9 | 3.4 | 3.7 | 0.69 |
| <i>Andesite</i> | | | | | | | | | | | | | | | |
| A87 | 6.2 | 338 | 0.0184 | 0.704738 | 10 | 0.70470 | 1.85 | 7.40 | 0.1518 | 0.512808 | 0.512757 | 9 | 3.3 | 3.6 | 0.78 |
| A89 | 15.1 | 314 | 0.0481 | 0.704784 | 11 | 0.70468 | 1.98 | 8.00 | 0.1503 | 0.512773 | 0.512723 | 9 | 2.6 | 2.9 | 0.84 |
| A94 | 10.3 | 304 | 0.0338 | 0.704579 | 10 | 0.70451 | 2.07 | 8.50 | 0.1479 | 0.512812 | 0.512762 | 9 | 3.4 | 3.7 | 0.73 |

Note: $\varepsilon_{\text{Nd}} = ((^{143}\text{Nd}/^{144}\text{Nd})_s / (^{143}\text{Nd}/^{144}\text{Nd})_{\text{CHUR}} - 1) \times 10,000$, $(^{143}\text{Nd}/^{144}\text{Nd})_{\text{CHUR}} = 0.512638$, and $(^{147}\text{Sm}/^{144}\text{Sm})_{\text{CHUR}} = 0.1967$ (Jacobsen and Wasserburg, 1980).

Nd single-stage and two-stage model ages (T_{DM}^* and T_{DM}^{**}) are calculated with a depleted-mantle reservoir and present-day values of $^{143}\text{Nd}/^{144}\text{Nd} = 0.513151$ and $^{147}\text{Sm}/^{144}\text{Sm} = 0.219$ (Liew and Hofmann, 1988).

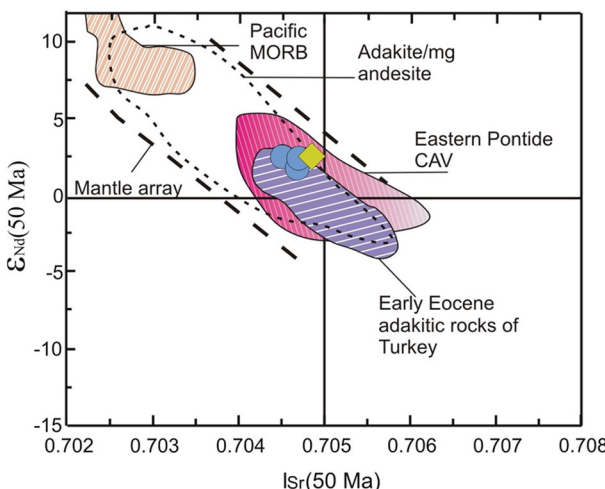


Fig. 9. Variation of lsr (50 Ma) versus ϵ_{Nd} (50 Ma) values. Fields for MORB and adakite/mg andesite from Castillo (2012), the Early Eocene adakitic rocks from Topuz et al. (2005, 2011), Karsli et al. (2010b, 2011), Eyuboglu et al. (2011a,c), and Dokuz et al. (2013), the Eastern Pontide calc-alkaline volcanic rocks (Arslan et al., 2013; Aydinçakir and Şen, 2013; Kaygusuz et al., 2011, Temizel et al., 2012) (symbols are as in Fig. 5a).

On the basis of $^{87}\text{Sr}/^{86}\text{Sr}$ versus Sr/Th relationships in a number of arcs, Hawkesworth et al. (1997) noted that high Sr/Th ratios are developed in rocks with low $^{87}\text{Sr}/^{86}\text{Sr}$ (~ 0.704). The rationale for using this plot is that as a result of the preferential mobilization of the LILE into hydrous fluids, high Sr/Th ratios will be a signature of the fluid phase. The Sr isotope ratios might be expected to be variable, depending on whether the fluids have interacted mainly with altered basaltic crust (≥ 0.7047 ; Bickle and Teagle, 1992; Staudigel et al., 1995) or subducted sediment (> 0.709). This indicates that the fluid components had similarly low $^{87}\text{Sr}/^{86}\text{Sr}$. Rocks from depleted and enriched arcs show (Fig. 13a) a hyperbola that implies that high Sr/Th (and thus, LILE/HFSE) ratios are better developed in the more depleted arc rocks, whereas low Sr/Th is accompanied by high $^{87}\text{Sr}/^{86}\text{Sr}$. The volcanic rocks span an array ($Sr/Th > 200$; $^{87}\text{Sr}/^{86}\text{Sr} < 0.705$) similar to that of depleted arcs, and show evidence for a considerable fluid input to their sources. Pb is fluid mobile like Sr, whereas Nd is fluid immobile and

this accounts for the vertical correlation of Pb/Nd versus Nd isotope ratios (Fig. 13b). The positive correlation between Th/Nd and Pb/Nd (Fig. 13c) shows that Pb and Th were affected similarly by subduction flux. There is an obvious vertical correlation between Gd/Yb and Th/Yb ratios of the non-adakitic volcanic rocks (Fig. 13d), indicating that the addition of slab fluids into the mantle wedge was in the form of an aqueous fluid rather than a slab melt.

The volcanic rocks represent somewhat high and flat HREE patterns (Fig. 8). This would normally indicate that the protolith may be garnet rich and would leave garnet-rich residue after melt extraction. Instead, the patterns are consistent with the property of spinel in the mantle source. The source enrichment features in the rocks may be examined in the Th/Yb versus Ta/Yb (Pearce et al., 1990, Fig. 14) diagram. In this diagram, the rocks form a trend sub-parallel to the mantle array, but shifted to higher Th/Yb ratios. This suggests a melt derivation from a source which itself had been previously enriched (or metasomatized) by fluids derived from an earlier (i.e., pre-Eocene) subduction process (e.g., Arslan et al., 2013; Aydinçakir and Şen, 2013). Bradshaw and Smith (1994) and Smith et al. (1999) implied that because HFSE (such as Nb and Ta) are depleted in the lithospheric mantle relative to the LREE, high Nb/La ratios (~ 1) indicate an OIB-like asthenospheric mantle source for basaltic magmas, and lower ratios (~ 0.5) indicate a lithospheric mantle source. The Nb/La (0.25–0.39) and La/Yb (2–6) ratios of the non-adakitic volcanic rocks in the Artvin area suggest a lithospheric mantle source. Their Ce/Pb (3–18) ratios differ from those of oceanic basalts (~ 25 ; Hofmann, 1997), indicating that asthenospheric mantle melts were not likely the source. The plot of La/Sm versus Sm/Yb distinguishes between melting of garnet and spinel peridotite sources. All the samples plot along the batch-melting curve of spinel peridotite (Fig. 15). REE modeling indicates that the non-adakitic volcanic rocks formed by spinel peridotite sources.

The Sr and Nd isotope ratios of the rocks define a narrow field between those of bulk earth composition and depleted mantle (Fig. 9). The isotope ratios are very close to those of Eastern Pontides calc-alkaline volcanics (Arslan et al., 2013; Aydinçakir and Şen, 2013; Kaygusuz et al., 2011; Temizel et al., 2012). On the basis of the combined trace elements and the Sr-Nd isotope data, we concluded that the parental magma of the volcanic rocks was derived from the partial melting of an enriched lithospheric mantle, which had been previously metasomatized by fluids derived from oceanic crust during previous subduction processes.

6. Geodynamic scenario for the non-adakitic volcanic rocks

The Eastern Pontides were affected by a complex tectonic regime since the late Paleocene–early Eocene (Okay and Şahintürk, 1997), and constitute an upper Mesozoic–early Tertiary east–west-trending magmatic belt (Fig. 1a). This belt is interpreted as an Andean type island arc developed in response to the northward subduction of the northern branch of Neotethys, resulting in the convergence of the Pontides in the north and the Tauride–Anatolide platform in the south (Okay and Şahintürk, 1997; Yilmaz et al., 1997a, 1997b). The closure of the Neotethyan Ocean was caused by a collision between the Pontide arc and the Tauride–Anatolide platform (Şengör and Yilmaz, 1981) (Fig. 16a, b). Both the onset of subduction and the timing of the collision between the Pontides and the Tauride–Anatolide platform are a matter of debate (Akin, 1979; Boztug et al., 2004; Karsli et al., 2011; Robinson et al., 1995; Tokel, 1977; Topuz et al., 2011). During the Paleocene–Early Eocene time, the Eastern Pontides were above sea level (Okay and Şahintürk, 1997), but based on structural data and the composition and timing of igneous activity, some authors (Boztug et al., 2006, 2007; Karsli et al., 2011; Okay and Şahintürk, 1997; Şengör and Yilmaz, 1981; Topuz et al., 2005, 2011; Yilmaz et al., 1997a, 1997b) propose a Paleocene–Early Eocene (ca. 55 Ma) collision, resulting in crustal thickening and the regional uplift of the Eastern Pontides. Robinson et al. (1995) and Tokel (1977) considered that the Middle Eocene volcanic

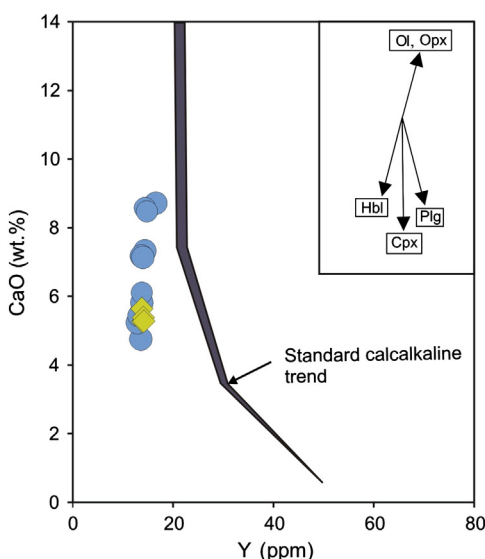


Fig. 10. CaO (wt.%) versus Y (ppm) plot for the studied volcanic rocks. Shaded area represents the “standard” calc-alkaline trend of Lambert and Holland (1974). The vectors show qualitative trends of the effect of fractional crystallization of common silicates (symbols are as in Fig. 5a).

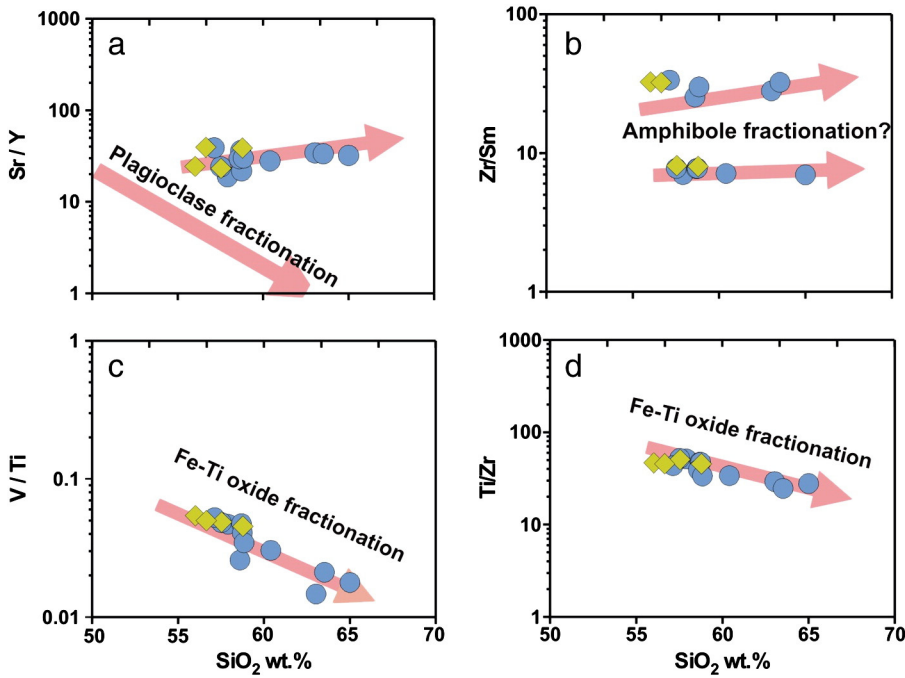


Fig. 11. Whole rock trace-element ratios (log scale) plotted vs. silica for volcanic rocks from the Artvin area. (a) Sr/Y reflects plagioclase fractionation within volcanics, (b) variation in Zr/Sm is often attributed primarily to amphibole fractionation. However, clinopyroxene and magnetite fractionation may also exert an influence on this ratio, (c,d) V/Ti and Ti/Zr variation show a strong signature of Fe-Ti oxide fractionation, but also may have been affected by amphibole fractionation (symbols are as in Fig. 5a).

rocks formed during the northward subduction of the Eastern Pontides and the subsequent collision occurred in the Oligocene (ca. 30 Ma). A different model (Eyüboğlu et al., 2011b, 2011c) showed that Eocene volcanic rocks were generated by slab window-related processes during ridge subduction in a south-dipping subduction zone.

There is significant consensus about the Eocene magmatism in the Pontides formed during a post-collisional, extensional geodynamic setting (Arslan et al., 2013; Aydin et al., 2008; Aydinçakir and Şen, 2013; Boztuğ and Harlavan, 2008; Boztuğ et al., 2004; Karsli et al., 2007, 2012; Temizel et al., 2012; Topuz et al., 2005, 2011; Yilmaz and Boztuğ, 1996; Yilmaz et al., 1997a, 1997b). Characteristics of isotopic analysis and the whole-rock geochemistry of the Early Eocene non-adakitic volcanic rocks indicate that the parental magmas were derived from a partial melting of an enriched lithospheric mantle. The partial melting of the lithospheric mantle could be due to two different reasons. These are (1) due to the adiabatic decompression resulting from the uplift of a slab break-off, and (2) because of an increase in heat from the upwelling asthenospheric mantle.

Four different models were proposed for the dynamic mechanism during the post-collisional setting: (1) slab break-off (Davies and von Blanckenburg, 1995; Kohn and Parkinson, 2002), (2) delamination of the lithosphere (Bird, 1979; Kay and Kay, 1993), (3) convective removal of the lithosphere (Houseman et al., 1981), and (4) intra-continental subduction (Arnaud et al., 1992; Tapponier et al., 2001). In all four models, asthenospheric upwelling is the main heat source for the partial melting. In the case of the Early Eocene non-adakitic volcanic rocks from the region, a generation from an enriched lithospheric mantle is documented by major and trace element features, $\text{Mg}\#$, Sr-Nd isotope characteristics, weak negative Eu anomalies, positive ϵ_{Nd} (t) values, and homogenous and low I_{Sr} (50 Ma) values (~0.704) of the samples. The last three models do not notably account for the generation of Early Eocene non-adakitic volcanic rocks. The collision took place between the Eastern Pontide and Anatolide-Tauride platform in the Paleocene (Okay and Şahintürk, 1997; Şengör and Yilmaz, 1981). The delamination process can not possibly be seen for the Eastern Pontides for a few reasons. First, the crustal thickness should be about twice of

normal thickness (~70 km, Molnar, 1990) after collision. Such a crustal thickness can be achieved as the result of the continent–continent collision by thrust stacking and shortening. The Paleocene collision occurred between two small continental blocks (e.g., the Eastern Pontides and the Anatolide-Tauride Block). Second, the time span of 10–15 Ma between initiation of collision and the first appearance of adakitic and non-adakitic magmatism (Late Paleocene–Early Eocene) in the Eastern Pontides was not enough to provide crustal thickening up to 70 km. Eocene structural and geophysical evidence are lacking for intra-continental subduction in the region. In the region, an active subduction is not a case during Early Eocene time. There is no known arc magmatism younger than 65 Ma in the Eastern Pontides although some researchers have interpreted the Middle Eocene igneous activity as subduction-related (Eyüboğlu et al., 2011c; Ustaömer et al., 2010). Following igneous activity occurred between 52 and 40 Ma and geochemical and isotopic signatures typical post-collisional rather than for subduction-related rocks (Arslan and Aslan, 2006; Arslan et al., 2013; Aydinçakir and Şen, 2013; Karsli et al., 2012). Existing age data of the Eastern Pontides express a ~13 Ma period of magmatic stagnation between the final subduction-related products and those formed during the following collisional periods. In contrast, the slab break-off model is more probable because the evidences support its occurrence in northwest and north-central Turkey in the Early Eocene as a result of a series of continental collisions within the Neotethyan realm (Altunkaynak and Dilek, 2006; Dilek and Altunkaynak, 2007; Dilek et al., 2010; Keskin et al., 2008). In this context, the following scenario is proposed for the genesis of the Early Eocene adakitic and non-adakitic suite (Fig. 16). The subduction of the Neotethyan Ocean occurred through the Late Cretaceous (Fig. 16a), followed by the collision between the Pontides and Anatolide-Tauride platform in the Paleocene (Fig. 16b) and finally the slab break-off of the Neotethyan oceanic slab (Fig. 16c). The source, geochemical signature, and timing of the Early Eocene magmatism are so important because there is still an ongoing debate on the origin and tectonic setting of the Eocene magmas in the Eastern Pontides. In some of recent studies (Karsli et al., 2010b, 2011, 2013; Topuz et al., 2005, 2011) the adakitic rocks of the Eastern Pontides are believed to have

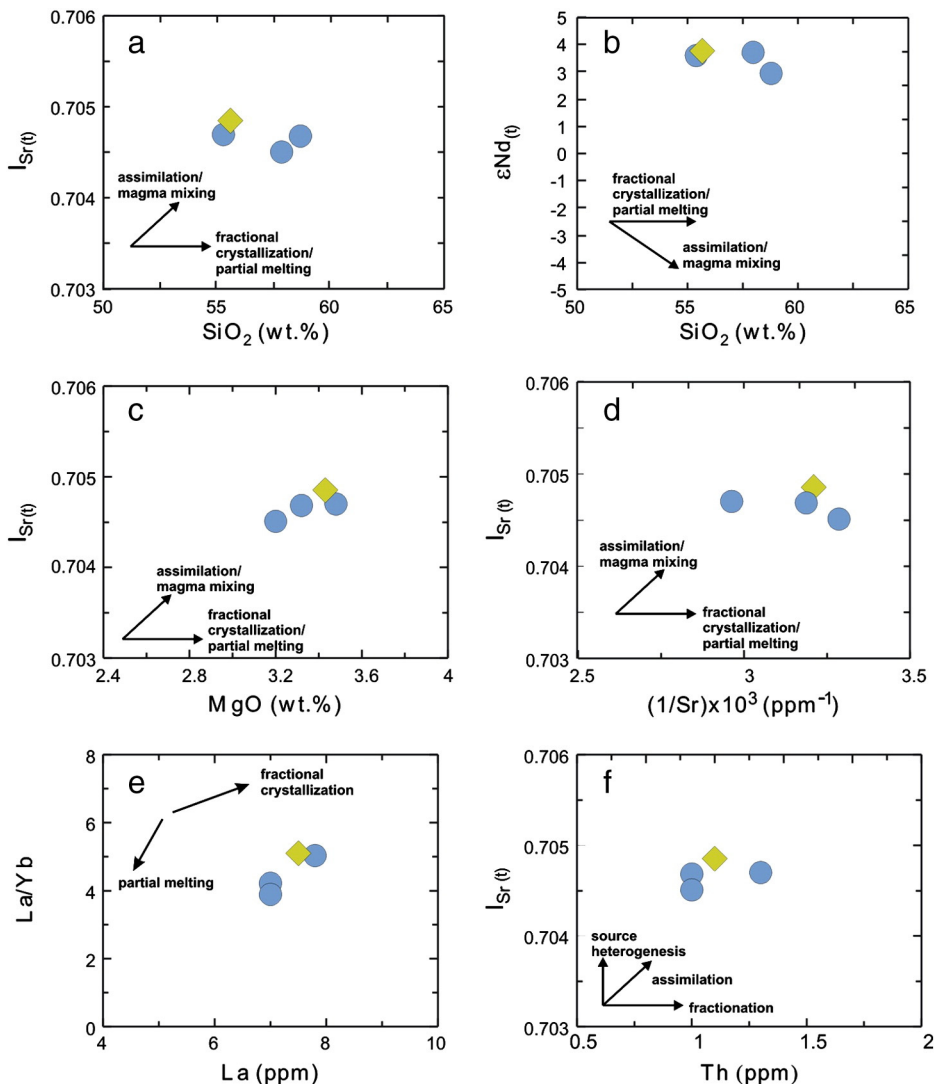


Fig. 12. (a) I_{Sr} (50 Ma) vs. SiO_2 (wt.%), (b) ϵ_{Nd} (50 Ma) vs. SiO_2 (wt.%), (c) I_{Sr} (50 Ma) vs MgO (wt.%), (d) I_{Sr} (50 Ma) vs. $(1/Sr) \times 10^3$ (ppm $^{-1}$), (e) La/Yb vs. La (ppm) and (f) I_{Sr} (50 Ma) vs Th (ppm) plots for the Early Eocene non-adakitic volcanic rocks from the Eastern Pontides (symbols are as in Fig. 5a).

formed by partial melting of thickened lower crust following the Paleocene collision of Pontides with the Tauride (Fig. 16c). However, oceanic slab melting during the slab break-off of the other model was proposed by Dokuz et al. (2013) for the origin of the adakitic rocks. On the other hand, according to a contrasting view these rocks were generated by slab window processes during ridge subduction in a south-dipping subduction zone (Eyuboglu et al., 2011a,c). The latter was thus an inevitable geodynamic event that occurred before the Middle Eocene. All of these events because they caused a loss of pressure over the asthenosphere, should have accelerated the asthenospheric uplift in the Early Eocene. This asthenospheric upwelling caused partial melting of the chemically-enriched sub-continental lithospheric mantle (SCLM) in a post-collisional setting in the Eastern Pontides throughout the Early Eocene (Fig. 16c).

7. Conclusions

The present study provides new constraints for the geodynamic evolution of the Eastern Pontides. The Early Eocene non-adakitic volcanism has not previously been reported in this region. Therefore, the petrogenetic and geodynamic processes of the Eastern Pontides are still debated. The results are as follows.

The Early Eocene non-adakitic volcanic rocks consist of andesite and trachy-andesite that display porphyric, microlitic porphyric, hyalomicrolitic porphyric, and glomeroporphyric textures. The rocks include hornblende ($Mg\# = 0.57\text{--}0.77$), plagioclase ($An_{14\text{--}69}$), and magnetite/Ti-magnetite. The ^{40}Ar - ^{39}Ar dating of the exhibits ages between 50.04 ± 0.10 and 50.47 ± 0.22 Ma (Ypresian). The volcanic rocks display tholeiitic to calc-alkaline character, with low and medium-K contents. All samples display similar geochemical features, which are characterized by the enrichment of LILE and LREE and depletion of HFSE without Eu anomalies, suggesting a similar parental magma and petrogenetic scenario. Fractional crystallization (FC) with minor contamination by upper crustal materials occurred during the evolution of the volcanic rocks. Hornblende, plagioclase, and Fe-Ti oxides were the most important fractionating mineral phases.

The Early Eocene non-adakitic volcanic rocks have narrow I_{Sr} (50 Ma) values varying between 0.70451 and 0.70485 and ϵ_{Nd} (50 Ma) values between 2.9 and 3.7. These isotopic features, in conjunction with their geochemical characters, suggest that the parental magma of the volcanic rocks originated from the melting of a young lithospheric mantle (T_{DM} is from 0.69 to 0.84 Ga), which was metasomatized by fluids derived from the subducted slab during the Early Cenozoic time. These rocks are

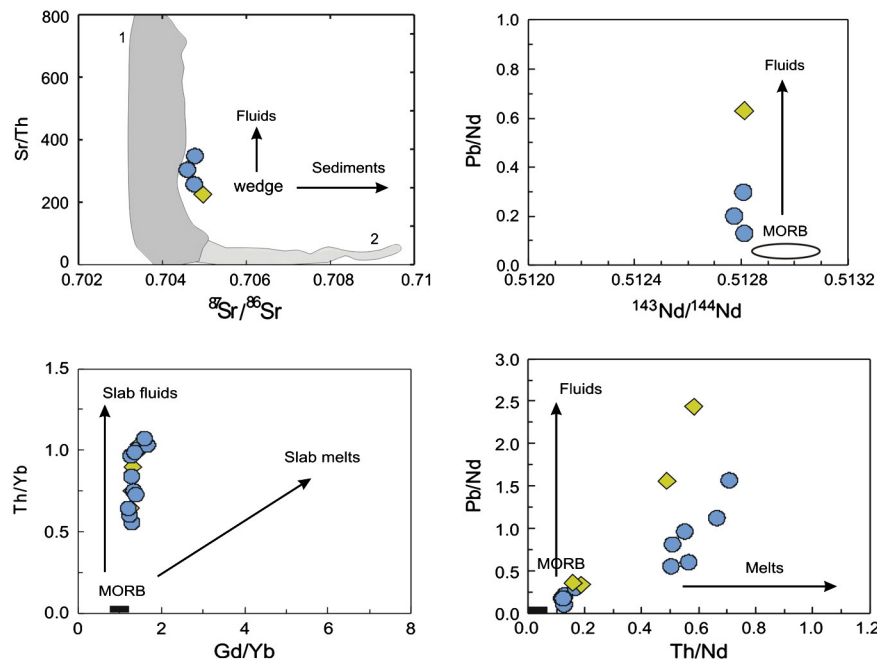


Fig. 13. (a) $^{87}\text{Sr}/^{86}\text{Sr}$ vs. Sr/Th variations in Early Eocene non-adakitic volcanic rocks. Fields 1 and 2 enclose data from arcs considered incompatible element depleted and enriched, respectively, by Hawkesworth *et al.* (1997). The arrows show the sense of enrichment predicted from addition of fluid and sedimentary components to the mantle wedge, (b) $^{143}\text{Nd}/^{144}\text{Nd}$ versus Pb/Nd, (c) Th/Nd versus Pb/Nd, and (d) Gd/Yb versus Th/Yb diagrams for the Early Eocene non-adakitic volcanic rocks. MORB values from Pearce and Parkinson (1993), (symbols are as in Fig. 5a).

considered to have been produced by partial melting of the lithospheric mantle in response to hot upwelling of the asthenosphere, possibly triggered by the break-off of the oceanic slab in a post-collision uplift phase representing compression in the Eastern Pontides.

Acknowledgments

This study was financially supported by the Scientific Research Foundation of Karadeniz Technical University (Project#: 2008.112.005.5). I

appreciate the help of Frank C. Ramos (New Mexico State University) during isotope analyses and Matthew T. Heizler (New Mexico Tech University) for $^{40}\text{Ar}/^{39}\text{Ar}$ geochronology analyses. The author thanks Ş. Can Genç and an anonymous reviewer for their accurate and constructive reviews. Editorial handling by Professor Nelson Eby is also highly appreciated. Thanks are due to Mürşid Öztürk and Hüseyin Asan for their assistances during field work.

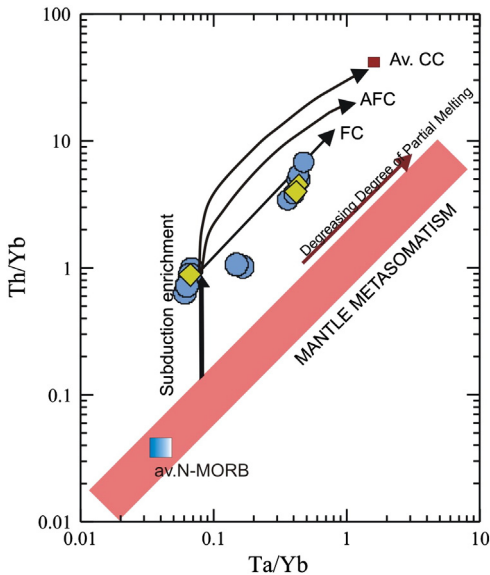


Fig. 14. Th/Yb versus Ta/Yb diagram (after Pearce et al., 1990) for the volcanic rocks. Average N-MORB composition and average Continental Crust (C) are from Sun and McDonough (1989) and Taylor and McLennan (1985), respectively. Vectors show that inferred effects of fractional crystallization (FC), assimilation-fractional crystallization (AFC), subduction enrichment and mantle metasomatism are from Pearce et al. (1990) (symbols are as in Fig. 5a).

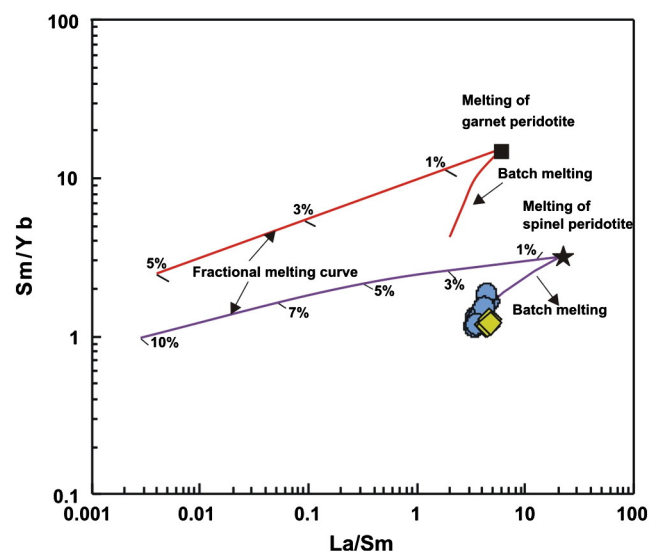


Fig. 15. La/Sm vs. Sm/Yb diagram showing the melting curves of the samples from the Artvin area. Fractional and batch melting equations of Shaw (1970) were used to construct the melting model. Modal mineralogy for the spinel- and garnet-peridotites are taken from Wilson (1989), and ol₆₆ + opx₂₄ + cpx₀₈ + sp₀₂ and ol₆₃ + opx₃₀ + cpx₀₂ + gt₀₅ respectively (ol: olivine, opx: orthopyroxene, cpx: clinopyroxene, sp: spinel, gt: garnet). Trace element composition of the spinel-peridotite (C_0 values) is from McDonough (1990), while that of garnet peridotite is from Frey (1980). K_{ds} between the basaltic melts and minerals given in the inset are compiled from Irving and Frey (1978), Fujimaki et al. (1984), McKenzie and O'Nions (1991) and Rollinson (1993) (symbols are as in Fig. 5a).

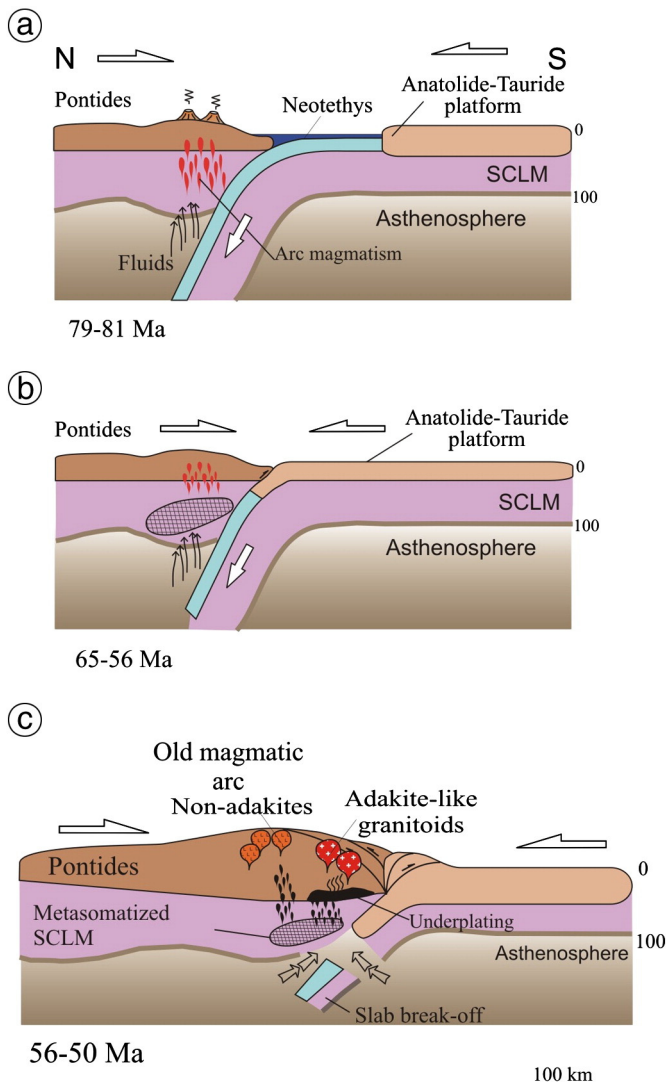


Fig. 16. Schematic diagram showing the tectonic evolution of the area studied between 81 and 50 Ma (a–c) and magmatic activity at ~50 Ma in Eastern Pontides, NE Turkey.

Appendix A. Supplementary data

Supplementary data to this article can be found online at <http://dx.doi.org/10.1016/j.lithos.2014.08.019>.

References

- Akin, H., 1979. Geologie, Magmatismus und Lager-staettenbildung im ostpontischen Gebirge-Turkei aus der Sicht der Plattentektonik. *Geologische Rundschau* 68, 253–283.
- Al'meev, R.R., Ariskin, A.A., Ozerov, A.Y., Kononkova, N.N., 2002. Problems of the stoichiometry and thermobarometry of magmatic amphiboles: an example of hornblende from the andesites of Bezymyanny Volcano, eastern Kamchatka. *Geochemistry International* 8, 803–819.
- Altherr, R., Topuz, G., Siebel, W., Şen, C., Meyer, H.P., Satir, M., Lahaye, Y., 2008. Geochemical and Sr-Nd-Pb isotopic characteristics of Paleocene plagioclaseites from the Eastern Pontides (NE Turkey). *Lithos* 105, 149–161.
- Altunkaynak, Ş., Dilek, Y., 2006. Timing and nature of postcollisional volcanism in western Anatolia and geodynamic implications. In: Dilek, Y., Pavlides, S. (Eds.), Postcollisional Tectonics and Magmatism in the Mediterranean region and Asia. Geological Society of America, Special Paper 409, pp. 321–351.
- Arnaud, N., Vidal, P., Tappognier, P., Matte, P., Deng, W.M., 1992. The high K₂O volcanism of northwestern Tibet: geochemistry and tectonic implications. *Earth and Planetary Science Letters* 111, 351–367.
- Arslan, M., Aslan, Z., 2006. Mineralogy, petrography and whole-rock geochemistry of the Tertiary granitic intrusions in the Eastern Pontides, NE Turkey. *Journal of Asian Earth Sciences* 27, 177–193.
- Arslan, M., Tüysüz, N., Korkmaz, S., Kurt, H., 1997. Geochemistry and petrogenesis of the Eastern Pontide volcanic rocks, northeast Turkey. *Chemie der Erde* 57, 157–187.
- Arslan, M., Temizel, İ., Abdioğlu, E., Kolaylı, H., Yücel, C., Boztug, D., Şen, C., 2013. ⁴⁰Ar/³⁹Ar dating, whole-rock and Sr-Nd-Pb isotopic geochemistry of post-collisional Eocene volcanic rocks in the southern part of the Eastern Pontides (NE Turkey): implications for magma evolution in extension-induced origin. *Contributions to Mineralogy and Petrology* 166, 113–142.
- Asan, K., Kurt, H., Francis, D., Morgan, G., 2014. Petrogenesis of the late Cretaceous K-rich volcanic rocks from the Central Pontide orogenic belt, North Turkey. *Island Arc* 23 (2), 102–124.
- Aslan, Z., 2010. U-Pb zircon SHRIMP age, geochemical and petrographical characteristics of tuffs within calc-alkaline Eocene volcanics around Gümüşhane (NE Turkey), Eastern Pontides. *Neues Jahrbuch für Mineralogie* 187 (3), 329–346.
- Aslan, Z., Arslan, M., Temizel, İ., Kaygusuz, A., 2014. K-Ar age, whole rock, and Sr-Nd isotope geochemistry of calc-alkaline volcanic rocks around the Gümüşhane area (Northeast Turkey): implications for post-collisional volcanism during Tertiary time in the Eastern Pontides. *Mineralogy and Petrology* 108, 245–267.
- Aydin, F., 2014. Geochronology, geochemistry, and petrogenesis of the Maçka subvolcanic intrusion: implications for the Late Cretaceous magmatic and geodynamic evolution of the eastern part of the Sakarya Zone, northeastern Turkey. *International Geology Review* 56 (10), 1246–1275.
- Aydin, F., Karsli, O., Chen, B., 2008. Petrogenesis of the Neogene alkaline volcanics with implications for post collisional lithospheric thinning of the Eastern Pontides, NE Turkey. *Lithos* 104, 249–266.
- Aydinçakir, E., 2012. Petrography, geochemistry and petrogenesis of the Borçka (Artvin, NE Turkey) area tertiary volcanics PhD thesis Karadeniz Technical University, Trabzon (200 pp.).
- Aydinçakir, E., Şen, C., 2013. Petrogenesis of the post-collisional volcanic rocks from the Borçka (Artvin) area: implications for the evolution of the Eocene magmatism in the Eastern Pontides (NE Turkey). *Lithos* 172–173, 998–117.
- Bacon, C.R., Hirschmann, M.M., 1988. Mg/Mn partitioning as a test for equilibrium between coexisting Fe-Ti oxides. *American Mineralogist* 73, 57–61.
- Baier, J., Audet, A., Kepler, H., 2008. The origin of the negative niobium tantalum anomaly in subduction zone magmas. *Earth and Planetary Science Letters* 267, 290–300.
- Bektas, O., Şen, C., Atıcı, Y., Köprübaşı, N., 1999. Migration of the Upper Cretaceous subduction-related volcanism toward the back-arc basin of the eastern Pontide magmatic arc (NE Turkey). *Geological Journal* 34, 95–106.
- Bektas, O., Çapkinoglu, Ş., Akdag, K., 2001. Successive extensional tectonic regimes during the Mesozoic as evidence by neptunian dykes in the Pontide Magmatic Arc, northeast Turkey. *International Geology Review* 43, 840–849.
- Bickle, M.J., Teagle, D.A.H., 1992. Strontium alteration in the Troodos ophiolite: implications for fluid fluxes and geochemical transport in mid-ocean ridge hydrothermal systems. *Earth and Planetary Science Letters* 113, 219–237.
- Bird, P., 1979. Continental delamination and the Colorado Plateau. *Journal of Geophysical Research* 84, 7561–7571.
- Boynton, W.V., 1984. Cosmochemistry of the rare earth elements: meteorite studies. In: Henderson, P. (Ed.), *Rare Earth Element Geochemistry*. Elsevier, Amsterdam.
- Bozta, D., Harlavan, Y., 2008. K-Ar ages of granitoids unravel the stages of Neo-Tethyan convergence in the Eastern Pontides and central Anatolia, Turkey. *International Journal of Earth Sciences* 97, 585–599.
- Bozta, D., Jonckheere, R.C., Wagner, G.A., Yeğençil, Z., 2004. Slow Senonian and fast Paleocene-Early Eocene uplift of the granitoids in the Central Eastern Pontides, Turkey: apatite fission-track results. *Tectonophysics* 382, 213–228.
- Bozta, D., Erçin, A.I., Kurugelik, M.K., Göç, D., Kömür, I., İskenderoğlu, A., 2006. Geochemical characteristics of the composite Kaçkar batholith generated in a Neo-Tethyan convergence system, Eastern Pontides, Turkey. *Journal of Asian Earth Sciences* 27, 286–302.
- Bozta, D., Jonckheere, R.C., Wagner, G.A., Erçin, A.I., Yeğençil, Z., 2007. Titanite and zircon fission-track dating resolves successive igneous episodes in the formation of the composite Kaçkar batholith in the Turkish Eastern Pontides. *International Journal of Earth Sciences* 96, 875–886.
- Bradshaw, T.K., Smith, E.I., 1994. Polygenetic Quaternary volcanism at Crater Flat, Nevada. *Journal of Volcanology and Geothermal Research* 63, 165–182.
- Cameron, B.I., Walker, J.A., Carr, M.J., Patino, L.C., Matias, O., Feigenson, M.D., 2003. Flux versus decompression melting at stratovolcanoes in southeastern Guatemala. *Journal of Volcanology and Geothermal Research* 119, 21–50.
- Çapkinoglu, Ş., 2003. First records of conodonts from the Permo-Carboniferous of Demirözü (Bayburt), Eastern Pontides, NE Turkey. *Turkish Journal of Earth Sciences* 12, 199–217.
- Castillo, P.R., 2012. Adakite petrogenesis. *Lithos* 134–135, 304–316.
- Davies, J.H., Von Blanckenburg, F., 1995. Slab breakoff: a model of lithospheric detachment and its test in the magmatism and deformation of collisional orogens. *Earth and Planetary Science Letters* 129, 85–102.
- Delaloye, M., Çögülu, E., Chessex, R., 1972. Etude géochronométrique des massifs cristallins de Rize et de Gümüşhane, Pontides Orientales Turquie. *Archives des Sciences Physiques et Naturelles* 25 (Suppl.7(2–3)), 43–52.
- Defant, M.J., Drummond, M.S., 1990. Derivation of some modern arc magmas by melting of young subducted lithosphere. *Nature* 347, 662–665.
- Dewey, J.F., Pitman, W.C., Ryan, W.B.F., Bonnin, J., 1973. Plate tectonics and evolution of the Alpine system. *Geological Society of America Bulletin* 84, 3137–3180.
- Dilek, Y., Altunkaynak, Ş., 2007. Cenozoic crustal evolution and mantle dynamics of post-collisional magmatism in western Anatolia. *International Geology Review* 49, 431–453.
- Dilek, Y., Imamverdiyev, N., Altunkaynak, Ş., 2010. Geochemistry and tectonics of Cenozoic volcanism in the Lesser Caucasus (Azerbaijan) and the peri-Arabian region:

- collision-induced mantle dynamics and its magmatic fingerprint. *International Geology Review* 52, 536–578.
- Dokuz, A., 2011. A slab detachment and delamination model for the generation of Carboniferous high-potassium I-type magmatism in the Eastern Pontides, NE Turkey: Kose composite pluton. *Gondwana Research* 19, 926–944.
- Dokuz, A., Tanyolu, E., 2006. Geochemical constraints on the provenance, mineral sorting and subaerial weathering of lower Jurassic and Upper Cretaceous clastic rocks from the Eastern Pontides, Yusufeli (Arvin), NE Turkey. *Turkish Journal of Earth Sciences* 15, 181–209.
- Dokuz, A., Karsli, O., Chen, B., Uysal, I., 2010. Sources and petrogenesis of Jurassic granitoids in the Yusufeli area, Northeastern Turkey: implications for pre- and post-collisional lithospheric thinning of the Eastern Pontides. *Tectonophysics* 480, 259–279.
- Dokuz, A., Uysal, I., Siebel, W., Turan, M., Duncan, R., Akçay, M., 2013. Post-collisional adakitic volcanism in the eastern part of the Sakarya Zone, Turkey: evidence for slab and crustal melting. *Contributions to Mineralogy and Petrology* 166, 1443–1468.
- Elburg, M.A., Bergen, M.V., Hoogewerff, J., Foden, J., Vroon, P., Zulkarmain, I., Nasution, A., 2002. Geochemical trends across an arc-continent collision zone: magma sources and slab-wedge transfer processes below the Panar Strait volcanoes, Indonesia. *Geochimica et Cosmochimica Acta* 66, 2771–2789.
- Eyüboğlu, Y., 2010. Late Cretaceous high-K volcanism in the Eastern Pontide orogenic belt, and its implications for the geodynamic evolution of NE Turkey. *International Geology Review* 52 (2–3), 142–186.
- Eyüboğlu, Y., Chung, S.L., Santosh, M., Dudas, F.O., Akaryali, E., 2011. Transition from shoshonitic to adakitic magmatism in the Eastern Pontides, NE Turkey: implications for slab window melting. *Gondwana Research* 19, 413–429.
- Eyüboğlu, Y., Santosh, M., Dudas, F.O., Chung, S.L., Akaryali, E., 2011. Migration magmatism in a continental arc: geodynamics of the Eastern Mediterranean revisited. *Journal of Geodynamics* 52, 2–15.
- Eyüboğlu, Y., Santosh, M., Chung, S.L., 2011a. Crystal fractionation of adakitic magmas in the crust–mantle transition zone: petrology, geochemistry and U–Pb zircon chronology of the Seme adakites, Eastern Pontides, NE Turkey. *Lithos* 121, 151–166.
- Eyüboğlu, Y., Santosh, M., Bektaş, O., Chung, S.L., 2011b. Late Triassic subduction-related ultramafic–mafic magmatism in the Amasya region (eastern Pontides, N. Turkey). *Journal of Asian Earth Sciences* 42, 234–257.
- Eyüboğlu, Y., Santosh, M., Yi, K., Bektaş, O., Kwon, S., 2012. Discovery of Miocene dakinite dacite from the Eastern Pontides Belt and revised geodynamic model for the late Cenozoic Evolution of eastern Mediterranean region. *Lithos* 146–147, 218–232.
- Frey, F.A., 1980. The origin of pyroxenites and garnet pyroxenites from salt lake crater, Oahu, Hawaii: trace element evidence. *American Journal of Science* 280, 427–449.
- Fujimaki, H., Tatsumoto, M., Aoki, K., 1984. Partition coefficients of Hf, Zr and REE between phenocrysts and groundmasses. Proceeding of the Fourteenth Lunar and Planetary Science Conference. Part 2. *Journal Geophysical Research Supplementary* 662–672.
- Genç, Ş.C., Tüysüz, O., 2010. Tectonic setting of the Jurassic bimodal magmatism in the Sakarya Zone (Central and Western Pontides), Northern Turkey: a geochemical and isotopic approach. *Lithos* 118, 95–111.
- Genç, S.C., Gulmez, F., Karacik, Z., Tuysuz, O., Prelevic, D., Roden, M.F., Hames, W.E., Billor, M.Z., 2014. Subduction-related high-to-ultrahigh-potassium rocks of the Ankara–Erzincan Suture Belt of Turkey: a geochemical and isotopic approach to source and petrogenesis. *Geophysical Research Abstracts Vol. 16. EGU General Assembly*.
- Giret, A., Bonin, B., Leger, J.M., 1980. Amphibole compositional trends in oversaturated and undersaturated alkaline plutonic ring complexes. *Canadian Mineralogist* 18, 481–495.
- Gülmez, F., Genç, C., Prelevic, D., 2014. Petrology and geochemistry of Late Cretaceous lamprophyric rocks from North Anatolian Ophiolitic Melange–Turkey. *Geophysical Research Abstracts Vol. 16. EGU General Assembly*.
- Hastie, A.R., Kerr, A.C., Pearce, J.A., Mitchell, S.F., 2007. Classification of altered volcanic island arc rocks using immobile trace elements: development of the Th–Co discrimination diagram. *Journal of Petrology* 48 (12), 2341–2357.
- Hawkesworth, C.J., Hergt, J.M., McDermott, F., Ellam, R.M., 1991. Destructive margin magmatism and the contributions from the mantle wedge and subducted crust, *Australian Journal of Earth Sciences* 38, 577–594.
- Hawkesworth, C.J., Turner, S., McDermott, F., Peate, D., Van Calsteren, P., 1997. U–Th isotopes in arc magmas: implications for element transfer from the subducted crust. *Science* 276, 551–555.
- Hofmann, A.W., 1997. Chemical differentiation of the Earth: the relationship between mantle, continental crust and oceanic crust. *Earth and Planetary Science Letters* 90, 297–314.
- Houseman, G.A., McKenzie, D.P., Molnar, P., 1981. Convective instability of a thickened boundary layer and its relevance for the thermal evolution of the continental convergent belt. *Journal of Geophysical Research* 86, 6115–6132.
- Irving, A.J., Frey, F.A., 1978. Distributions of trace elements between garnet megacrysts and host volcanic liquids of kimberlitic to rhyolitic composition. *Geochimica et Cosmochimica Acta* 42, 771–787.
- Jacobsen, S.B., Wasserburg, G.J., 1980. Sm–Nd isotopic evolution of chondrites. *Earth and Planetary Science Letters* 50, 139–155.
- Kandemir, R., 2004. Sedimentary characteristics and depositional conditions of Lower–Middle Jurassic Şenköy Formation in the around of Gümüşhane, Unpublished PhD thesis. Karadeniz Technical University, Trabzon, Turkey, 274 pp.
- Kandemir, R., Yılmaz, C., 2009. Lithostratigraphy, facies, and deposition environment of the lower Jurassic Ammonitico Rosso type sediments (ARTS) in the Gümüşhane, area, NE Turkey: implications for the opening of the northern branch of the Neo-Tethys Ocean. *Journal of Asian Earth Sciences* 34, 586–598.
- Karsli, O., Chen, B., Aydin, F., Şen, C., 2007. Geochemical and Sr–Nd–Pb isotopic compositions of the Eocene Dölek and Sarıçek Plutons, Eastern Turkey: implications for magma interaction in the genesis of high-K calc-alkaline granitoids in a post-collision extensional setting. *Lithos* 98, 67–96.
- Karsli, O., Dokuz, A., Uysal, I., Aydin, F., Bin, C., Kandemir, R., Wijbrans, J.R., 2010a. Relative contributions of crust and mantle to generation of Campanian high-K calc-alkaline I-type granitoids in a subduction setting, with special reference to the Harşit pluton, Eastern Turkey. *Contribution to Mineralogy and Petrology* 160, 467–487.
- Karsli, O., Dokuz, A., Uysal, I., Aydin, F., Kandemir, R., Wijbrans, J.R., 2010b. Generation of the Early Cenozoic adakitic volcanism by partial melting of mafic lower crust, Eastern Turkey: implication for crustal thickening to delamination. *Lithos* 114, 109–120.
- Karsli, O., Uysal, I., Ketenci, M., Dokuz, A., Aydin, F., Chen, B., Kandemir, R., Wijbrans, J., 2011. Adakite-like granitoid porphyries in Eastern Pontides, NE Turkey: potential parental melts and geodynamic implications. *Lithos* 127, 354–372.
- Karsli, O., Dokuz, A., Uysal, I., Ketenci, M., Chen, B., Kandemir, R., 2012. Deciphering the shoshonitic monzonites with I-type characteristics, the Sıdağı pluton, NE Turkey: magmatic response to continental lithospheric thinning. *Journal of Asian Earth Sciences* 51, 45–62.
- Karsli, O., Uysal, I., Dilek, Y., Aydin, F., Kandemir, R., 2013. Geochemical modelling of early Eocene adakitic magmatism in the Eastern Pontides, NE Anatolia: continental crust or subducted oceanic slab origin? *International Geology Review* 55 (16), 2085–2095.
- Karsli, O., Dokuz, A., Kaliwoda, M., Uysal, I., Aydin, F., Kandemir, R., Fehr, K.T., 2014. Geochemical fingerprints of Late Triassic calc-alkaline lamprophyres from the Eastern Pontides, NE Turkey: a key to understanding lamprophyre formation in subduction-related environment. *Lithos* 196–197, 181–197.
- Kay, R.W., Kay, S.M., 1993. Delamination and delamination magmatism. *Tectonophysics* 219, 177–189.
- Kaygusuz, A., Aydinçakır, E., 2009. Mineralogy, whole rock and Sr–Nd isotope geochemistry of mafic microgranular enclaves in Cretaceous Dağbaşı granitoids, eastern Pontides, NE Turkey: evidence of magma mixing, mingling, and chemical equilibration. *Chemie der Erde–Geochemistry* 69, 247–277.
- Kaygusuz, A., Aydinçakır, E., 2011. U–Pb zircon SHRIMP ages, geochemical and Sr–Nd isotopic compositions of Cretaceous plutons in the eastern Pontides (NE Turkey): the Dağbaşı pluton. *Neues Jahrbuch für Mineralogie* 188 (3), 211–233.
- Kaygusuz, A., Arslan, M., Siebel, W., Şen, C., 2011. Geochemical and Sr–Nd isotopic characteristics of post-collision calc-alkaline volcanics in the Eastern Pontides (NE Turkey). *Turkish Journal of Earth Sciences* 20, 137–159.
- Kaygusuz, A., Arslan, M., Siebel, W., Sipahi, F., İlbeyle, N., 2012. Geochronological evidence and tectonic significance of Carboniferous magmatism in southwest Trabzon area, eastern Pontides, Turkey. *International Geology Review* 54 (5), 1776–1800.
- Keskin, M., Genç, Ş.C., Tüysüz, O., 2008. Petrology and geochemistry of postcollisional Middle Eocene volcanic units in North-Central Turkey: evidence for magma generation by slab breakoff following the closure of the Northern Neotethys Ocean. *Lithos* 104, 267–305.
- Kohn, M.J., Parkinson, C.D., 2002. Petrologic case for Eocene slab breakoff during the Indo-Asian collision. *Geology* 30, 591–594.
- Kuiper, K.F., Deino, A., Hilgen, F.J., Krijgsman, W., Renne, P.R., Wijbrans, J.R., 2008. Synchronizing the rock clocks of Earth history. *Science* 320, 500–504.
- Lambert, R.J., Holland, J.G., 1974. Yttrium geochemistry applied to petrogenesis utilizing calcium–yttrium relationships in minerals and rocks. *Geochimica et Cosmochimica Acta* 38, 1393–1414.
- Le Bas, M.J., Le Maitre, R.W., Streckeisen, A., Zanettin, B., 1986. A chemical classification of volcanic rocks on the total alkali–silica diagram. *Journal of Petrology* 24 (3), 745–750.
- Leake, E.B., Wooley, A.R., Arps, C.E.S., Birch, W.D., Gilbert, M.C., Grice, J.D., Hawthorne, F.C., Kato, A., Kisch, H.J., Krivovichev, V.G., Linthout, K., Laird, J., Mandarino, J., Maresch, W.V., Nickel, E.H., Rock, N.M.S., Schumacher, J.C., Smith, D.C., Stephenson, N.C.N., Ungarotti, L., Whittaker, E.J.W., Youzhi, G., 2004. Nomenclature of amphiboles report of the subcommittee on amphiboles of the International Mineralogical Association Commission on New Minerals and Mineral Names. *European Journal of Mineralogy* 9, 623–651.
- Liew, T.C., Hofmann, A.W., 1988. Precambrian crustal components, plutonic associations, plate environment of the Hercynian Fold Belt of central Europe: indications from a Nd and Sr isotopic study. *Contributions to Mineralogy and Petrology* 98, 129–138.
- M.T.A., 2002. 1:500,000-Scale Map of Turkey, General Directorate of Mineral Research and Exploration (M.T.A.), Ankara, Turkey.
- McDonough, W.F., 1990. Constraints on the composition of the continental lithospheric mantle. *Earth and Planetary Science Letters* 101, 1–18.
- McKenzie, D.P., O’Nions, R.K., 1991. Partial melt distributions from inversion of rare earth element concentrations. *Journal of Petrology* 32, 1021–1091.
- Min, K., Mundil, R., Renne, P.R., Ludwig, K.R., 2000. A test for systematic errors in $^{40}\text{Ar}/^{39}\text{Ar}$ geochronology through comparison with U–Pb analysis of a 1.1 Ga rhyolite. *Geochimica et Cosmochimica Acta* 64, 73–98.
- Molnar, P., 1990. S-wave residuals from earthquakes in the Tibetan region and lateral variations in the upper mantle. *Earth and Planetary Science Letters* 101, 68–77.
- Münker, C., Wörner, G., Yıldız, G., Churikova, T., 2004. Behaviour of high field strength elements in subduction zones: constraints from Kamchatka–Aleutian arc lavas. *Earth and Planetary Science Letters* 224, 275–293.
- Nielsen, C.H., Sigurdsson, H., 1981. Quantitative methods for electron microprobe analysis of sodium in natural and synthetic glasses. *American Mineralogist* 66, 547–552.
- Nielsen, R.L., Forsythe, L.M., Gallahan, W.E., Fisk, M.R., 1994. Major and trace element magnetite–melt equilibria. *Chemical Geology* 117, 167–191.
- Okay, A., 1996. Granulite facies gneisses from the Pulur region, Eastern Pontides. *Turkish Journal of Earth Sciences* 5, 55–61.
- Okay, A.I., Tüysüz, O., 1999. Tethyan sutures of northern Turkey. *Geological Society of London, Special Publications* 156, 475–515.

- Okay, A.I., Şahintürk, Ö., 1997. Geology of the Eastern Pontides. In: Robinson, A.G. (Ed.), *Regional and Petroleum Geology of the Black Sea and Surrounding Region*. American Association of Petroleum Geologists (AAPG) Memoir 68, pp. 291–311.
- Pearce, J.A., 1983. Role of the sub-continental lithosphere in magma genesis at active continental margins. In: Hawkesworth, C.J., Norry, M.J. (Eds.), *Continental Basalts and Mantle Xenoliths*, Shiva, Cheshire, pp. 230–249.
- Pearce, J.A., Norry, M.L., 1979. Petrogenetic implications of Ti, Zr, Y, and Nb variations in volcanic rocks: Contributions to Mineralogy and Petrology 69, 33–47.
- Pearce, J.A., Parkinson, I.J., 1993. Trace element models for mantle melting: application to volcanic arc petrogenesis. In: Prichard, H.M., Alabaster, T., Harris, N.B.W., Neary, C.R. (Eds.), *Magmatic Processes and Plate Tectonics*. Geological Society London Special Publication 76, pp. 373–403.
- Pearce, J.A., Bender, J.F., De Long, S.E., Kidd, W.S.F., Low, P.J., Güner, Y., Saroğlu, F., Yilmaz, Y., Moorbat, S., Mitchell, J.J., 1990. Genesis of collision volcanism in eastern Anatolia Turkey. *Journal of Volcanology and Geothermal Research* 44, 189–229.
- Ramos, F.C., 1992. Isotope Geology of Metamorphic Core of the Central Grouse Creek Mountains, Box Elder County, Utah (MSC thesis) University of California, Los Angeles.
- Ringwood, A.E., 1990. Slab-mantle interactions: 3. petrogenesis of intra-plate magmas and structure of the upper mantle. *Chemical Geology* 82, 187–207.
- Robinson, A.G., Banks, C.J., Rutherford, M.M., Hirst, J.P., 1995. Stratigraphic and structural development of the eastern Pontides, Turkey. *Geological Society of London* 152, 861–872.
- Rollinson, H.R., 1993. *Using Geochemical Data: Evaluation, Presentation, Interpretation*, Longman Scientific and Technical. John Wiley and Sons, New York.
- Sakoma, E.M., Martin, R.F., Williams, Jones A.E., 2000. The late stages evolution of the Kwandonkaya A-type granite complex, Nigeria, as deduced from mafic minerals. *Journal of African Earth Sciences* 30, 329–350.
- Şen, C., 2007. Jurassic volcanism in the Eastern Pontides: is it rift related or subduction related? *Turkish Journal of Earth Sciences* 16, 523–539.
- Şen, C., Arslan, M., Van, A., 1998. Doğu Pontid (Kd Türkiye) Eosen (?) Alkalen Volkanik Provensinin Jeokimyasal ve Petrolojik Karakteristikleri, Tübıtak Yayınları. *Turkish Journal of Earth Sciences* 7, 231–239.
- Şengör, A.M.C., Yılmaz, Y., 1981. Tethyan evolution of Turkey: a plate tectonic approach. *Tectonophysics* 75, 181–241.
- Şengör, A.M.C., Özeren, S., Genç, T., Zor, E., 2003. East Anatolian high plateau as a mantle-supported, north-south shortened domal structure. *Geophysical Research Letters* 30 (24). <http://dx.doi.org/10.1029/2003gl017858>.
- Shaw, D.M., 1970. Trace element fractionation during anatexis. *Geochimica et Cosmochimica Acta* 34, 237–243.
- Smith, E.I., Sanchez, A., Walker, J.D., Wang, K., 1999. Geochemistry of mafic magmas in the Hurricane Volcanic field, Utah: implications for small and large scale chemical variability of the lithospheric mantle. *Journal of Geology* 107, 433–448.
- Staudigel, H., Davies, G.R., Hart, S.R., Marchant, K.M., Smith, B.M., 1995. Large scale isotopic Sr, Nd and O isotope anatomy of altered oceanic crust at DSDP7ODP sites 417/418. *Earth and Planetary Science Letters* 130, 169–185.
- Sun, S., McDonough, W.F., 1989. Chemical and isotopic systematics of oceanic basalt: implications for mantle composition and processes. In: Saunders, A.D., Norry, M.J. (Eds.), *Magmatism in the Ocean Basins*. Geological Society of London Special Publication 42, pp. 313–345.
- Tappognier, P., Xu, Z.Q., Roger, F., Meyer, B., Arnaud, N., Wittlinger, G., Yang, J.S., 2001. Oblique stepwise rise and growth of the Tibet plateau. *Science* 294, 1671–1677.
- Tatsumi, Y., Eggins, S.M., 1995. Subduction Zone Magmatism. Blackwall, Cambridge.
- Taylor, S.R., McLennan, S.M., 1985. *The continental crust. Its Composition and Evolution*. Blackwell, Oxford.
- Temizel, İ., Arslan, M., Ruffet, G., Peucat, J.J., 2012. Petrochemistry, geochronology and Sr–Nd isotopic systematic of the Tertiary collisional and post-collisional volcanic rocks from the Ulubey (Ordu) area, Eastern Pontide, NE Turkey: implications for extension-related origin and mantle source characteristics. *Lithos* 128, 126–147.
- Thirlwall, M.F., Smith, T.E., Graham, A.M., Theodorou, N., Hollings, P., Davidson, J.P., Arculus, R.J., 1994. High field strength element anomalies in arc lavas: source or process? *Journal of Petrology* 35 (3), 819–838.
- Thirlwall, M.F., Graham, A.M., Arculus, R.J., Harmon, R.S., Macpherson, C.G., 1996. Resolution of the effects of crustal assimilation, sediment subduction, and fluid transport in island arc magmas: Pb–Sr–Nd–O isotope geochemistry of Grenada, Lesser Antilles. *Geochimica et Cosmochimica Acta* 60, 4785–4810.
- Thompson, R.N., Morrison, M.A., Hendry, G.L., Parry, S.J., 1984. An assessment of the relative roles of crust and mantle in magma genesis: an elemental approach. *Philosophical Transactions of the Royal Society* 310, 549–590.
- Tokel, S., 1977. Doğu Karadeniz Bölgesi'nde Eosen Yaşı Kalkalkalen Andezitler ve Jeotektonizma. *Türkiye Jeoloji Kurumu Bülteni* 20, 49–54.
- Topuz, G., Alther, R., Schwarz, W.H., Siebel, W., Satır, M., Dokuz, A., 2005. Postcollisional plutonism with adakite-like signatures: the Eocene Sarayçık granodiorite (Eastern Pontides, Turkey). *Contributions to Mineralogy and Petrology* 150, 441–455.
- Topuz, G., Alther, R., Schwarz, W.H., Dokuz, A., Meyer, H.P., 2007. Variscan amphibolite-facies rocks from the Kurtoglu metamorphic complex, Gümüşhane area, Eastern Pontides, Turkey. *International Journal of Earth Sciences* 96, 861–873.
- Topuz, G., Alther, R., Wolfgang, S., Schwarz, W.H., Zack, T., Hasanözbek, A., Mathias, B., Satır, M., Şen, C., 2010. Carboniferous high-potassium I-type granitoid magmatism in the Eastern Pontides: the Gümüşhane pluton (NE Turkey). *Lithos* 116, 92–110.
- Topuz, G., Okay, A.I., Alther, R., Schwarz, W.H., Siebel, W., Zack, T., Satır, M., Şen, C., 2011. Post-collisional adakite-like magmatism in the Ağvaniş massif and implications for the evolution of the Eocene magmatism in the Eastern Pontides (NE Turkey). *Lithos* 125, 131–150.
- Tribuzio, R., Tiepolo, M., Vannucci, R., Bottazzi, P., 1999. Trace element distribution within olivine-bearing gabbros from the Northern Apennine ophiolites (Italy): evidence for post-cumulus crystallization in MOR-type gabbroic rocks. *Contributions to Mineralogy and Petrology* 134, 123–133.
- Ustaömer, T., Robertson, H.F.A., 2010. Late Paleozoic–Early Cenozoic development of the Eastern Pontides (Artvin area), Turkey: stages of closure of Tethys along the southern margin of Eurasia. *Geological Society, London, Special Publications* 340, 281–327.
- Van, A., 1990. *Pontid Kuşağı'nda Artvin Bölgesi'nin Jeokimyası, Petrojenezi ve Masif Sülfid Mineralizasyonları* (PhD thesis) Karadeniz Technical University, Trabzon.
- Wilson, M., 1989. *Igneous petrogenesis. A Global Tectonic Approach*. Harper Collins Academic, London (456 pp.).
- Winchester, J., Floyd, P.A., 1977. Geochemical discrimination of different magma series and their differentiation products using immobile elements. *Chemical Geology* 20, 325–343.
- Yilmaz, Y., 1972. Petrology and structure of the Gümüşhane granite and the surrounding rocks. NE Anatolia PhD Thesis University College London, England, p. 248.
- Yilmaz, S., Bozta, D., 1996. Space and time relations of three plutonic phases in the Eastern Pontides, Turkey. *International Geology Review* 38, 935–956.
- Yilmaz, A., Engin, T., Adami, S., Lazarashvili, T., 1997a. *Geoscientific Studies of the Area Along Turkish–Georgian Border*. MTA, Ankara.
- Yilmaz, Y., Tüysüz, O., Yiğitbaş, E., Genç, Ş.C., Şengör, A.M.C., 1997b. Geology and tectonic evolution of the Pontides. In: Robinson, A.G. (Ed.), *Regional and Petroleum Geology of the Black Sea and Surrounding Region*. American Association of Petroleum Geologists Memoir 68, pp. 183–226.
- Yücel, C., Arslan, M., Temizel, İ., Abdioglu, E., 2014. Volcanic facies and mineral chemistry of Tertiary volcanics in the northern part of the Eastern Pontides, northeast Turkey: implications for pre-eruptive crystallization conditions and magma chamber processes. *Mineralogy and Petrology* 108, 439–467.